MARMARA UNIVERSITY
INSTITUTE FOR GRADUATE STUDIES
IN PURE AND APPLIED SCIENCES

PREPARATION OF VEGETABLE OIL-BASED COATINGS BY UV INDUCED THIOL-ENE CLICK CHEMISTRY AND INVESTIGATION OF THEIR PROPERTIES

EDA GAŞ

MASTER THESIS
Department of Polymer Science and Technology

Thesis Supervisor
Prof. Dr. Nilhan KAYAMAN APOHAN

Co-Supervisor
Assoc. Prof. Dr. Burcu OKTAY

ISTANBUL, 2024

MARMARA UNIVERSITY
INSTITUTE FOR GRADUATE STUDIES
IN PURE AND APPLIED SCIENCES

PREPARATION OF VEGETABLE OIL-BASED COATINGS BY UV INDUCED THIOL-ENE CLICK CHEMISTRY AND INVESTIGATION OF THEIR PROPERTIES

EDA GAŞ
526620009

MASTER THESIS
Department of Polymer Science and Technology

Thesis Supervisor
Prof. Dr. Nilhan KAYAMAN APOHAN

Co-Supervisor
Assoc. Prof. Dr. Burcu OKTAY

ISTANBUL, 2024

PREFACE

I would like to begin by expressing my heartfelt gratitude to Prof. Dr. Nilhan Kayaman Apohan for her invaluable guidance and support throughout the completion of my Master's thesis. Her expertise, encouragement, and mentorship have been instrumental in shaping this study and enhancing my academic journey.

Also, I like to extend my sincere thanks to Assoc. Prof. Dr. Burcu Oktay for her patience, understanding, and encouragement during the research process. Her feedback and insights have been immensely valuable in improving the quality of this thesis during the laboratory process.

I would also like to express my sincere gratitude to Assoc. Prof. Dr. Emrah Çakmakçı for his support during the laboratory process.

In addition, I would like to thank my friends Mücahit Özdemir, Fatmanur Uyumaz, İlkay Güneş, Emel Atılal and Neslihan İşleyen for their moral support and encouragement during moments of doubt and difficulty. Their friendship and belief in me have been a source of strength and motivation throughout this academic endeavor.

Finally, I am grateful to my mother, father, and brother for their unwavering moral support throughout the thesis process.

March, 2024 **Eda GAŞ**

CONTENTS

PAGE

PREFACE ..... **i**
CONTENTS ..... **ii**
ÖZET ..... **v**
ABSTRACT ..... **vi**
SYMBOLS ..... **vii**
ABBREVIATIONS ..... **viii**
LIST OF FIGURES ..... **ix**
LIST OF TABLES ..... **xi**
1. GENERAL INFORMATION **1**
1.1. Extraction and Classification of Vegetable Oil 2
1.2. Structure and Properties of Vegetable Oil 3
1.2.1. Linseed oil 7
1.3. Chemical Modification of Vegetable Oil 8
1.3.1. Epoxidation of vegetable oil 10
1.3.2. Acrylation of vegetable oil 12
1.4. Coatings Prepared by UV Curing 14
1.4.1. Uv-curable system components 16
1.4.1.1. Photoinitiators 17
1.4.1.2. Reactive solvents 18
1.4.1.3. Reactive oligomers 19
1.4.2. Advantages and disadvantages of UV curable coatings 21
1.5. Click Chemistry 23
1.5.1. Thiol-ene click chemistry 24
1.5.1.1. Advantages and disadvantages of thiol-ene click chemistry 26
1.5.1.2. Thiol-ene coatings containing vegetable oils 27
1.5.1.3. Thiol-anhydride dynamic reversible networks 27
2. MATERIAL AND METHOD **29**
2.1. Chemicals and Materials Used 29
2.2. Devices and Equipment Used 33
2.2.1. Fourier transform infrared (FT-IR) spectroscopy 33

2.2.2. Nuclear magnetic resonance spectroscopy (1H-NMR) 33
2.2.3. Water contact angle..... 33
2.2.4. Tensile rupture test..... 33
2.2.5. Differential scanning calorimeter (DSC) 33
2.2.6. Thermogravimetric and differential thermal analyzer (TG/DTA)..... 34
2.2.7. Pencil hardness test..... 34
2.2.8. Cross-cut test 34
2.2.9. Pendulum test 34
2.3. Equipment..... 34
2.3.1. PTFE mold 34
2.3.2. Glass plate 35
3. EXPERIMENTAL METHOD..... 36
3.1. Synthesis of Epoxidized Linseed Oil (ELO) 36
3.2. Acrylation of Epoxidized Linseed Oil..... 36
3.3. Synthesis of Thiol Compound 37
3.4. Preparation of UV Curable Films with Thiol-Ene Click Chemistry..... 39
4. RESULTS AND DISCUSSION 42
4.1. FTIR Analysis of Epoxidized Linseed Oil 42
4.2. FTIR and ^{1}HNMR Analysis of Acrylization of ELO 44
4.3. FTIR and ^{1}HNMR Analysis of Thiol Compound..... 46
4.4. FTIR Analysis of Prepared Films 48
4.5. Performance Properties of Prepared Films..... 48
4.5.1. Differential scanning calorimetry device (DSC) 48
4.5.2. TG-DTA analysis of prepared films 51
4.5.3. Gel content of prepared films..... 52
4.5.4. Tensile test of prepared film..... 53
4.6. Physical and Mechanical Performance Properties of Coatings 54
4.6.1. Pendulum hardness test analysis..... 54
4.6.2. Pencil hardness 55
4.6.3. Contact Angle..... 55
4.6.4. Cross-Cut analysis 56
RESULTS..... 58

REFERENCES **61**
ADDITIONAL RESOURCES **70**
RESUME **74**

ÖZET

UV KAYNAKLI TİYOL-EN KLİK KİMYASI İLE BİTKİSEL YAĞ BAZLI KAPLAMALARIN HAZIRLANMASI VE ÖZELLİKLERİNİN İNCELENMESİ

UV ile kürlenebilen kaplamalar, daha az enerji tüketimi, minimum uçucu organik kimyasal (VOC) emisyonu, ekonomik sermaye yatırımlarına uygun olması ve ortam koşullarında bile hızlı kürlenme oranları gibi olağanüstü özelliklerinden dolayı büyük ilgi toplamıştır. Önceki yıllarda UV ile kürlenen hammaddelerin çoğunu hazırlamak için petrokimyasallar kullanılıyordu. Ancak petrokimya rezervlerinin tükenmesi ve bunların zararlı çevresel sonuçları, alternatif yaklaşımların gerekliliğini ortaya çıkardı. Bu nedenle son zamanlarda UV ile kürlenen kaplamalarda bitkisel yağların kullanılmasında bir artış yaşanmaktadır. Bu değişim, bitkisel yağların yenilenebilir doğasından, düşük toksisite profillerinden, yüksek uygulanabilirliğinden ve trigliserit yapılarının kaplama matrisinin ayrılmaz bileşenlerine kusursuz dönüşümünden kaynaklanmaktadır. Bu çalışmada, kaplamada çevre dostu bir bitkisel yağ olan ve diğer yağlara göre daha yüksek rektiviteye sahip olan keten tohumu yağı kullanıldı. İlk olarak, epoksidasyon işlemi ile oksiran halkası (epoksi grubu) keten tohumu yağ asidi zincirlerine bağlandı. Bu modifikasyonun ardından epoksi grupları, akrilik asit ile halka açma reaksiyonu yoluyla akrilasyona tabi tutuldu ve akrillenmiş epokside keten tohumu yağı (AELO) elde edildi. Ek olarak, bitkisel yağ bazlı tiyol-en kaplamaya dinamik kovalent bağlar sağlamak için 1,6-heksanditiyol ve maleik anhidrit kullanılarak hem tiyol hem de karboksilik asit gruplarını içeren fonksiyonel bir monomer sentezlendi.AELO, sentezlenen fonksiyonel tiyol bileşiği ve ticari 4 fonksiyonlu tiyol bileşiği olan pentaeritritol tetrakis (3-merkaptopropiyonat) farklı oranlarda hazırlanarak UV ışınları ile çapraz bağlandı. Tiyol-en klik kimyası ile elde edilen UV kaynaklı biyo bazlı filmler ve kaplamalar daha sonra postkür uygulamasıyla 1 saat 120 °C'de ve 24 saat 120 °C'de etüvde bekletildi. Elde edilen filmlerin kimyasal, mekanik, termal ve yüzey özellikleri incelendi. Aynı zamanda hazırlanan kaplamalar için performans testleri de gerçekleştirildi.

Mart, 2024 **Eda GAŞ**

ABSTRACT

PREPARATION OF VEGETABLE OIL-BASED COATINGS BY UV INDUCED THIOL-ENE CLICK CHEMISTRY AND INVESTIGATION OF THEIR PROPERTIES

UV-curable coatings have garnered significant interest due to their exceptional attributes, including reduced energy consumption, minimal emissions of volatile organic chemicals (VOCs), economical capital investments, and rapid curing rates even under ambient conditions. Petrochemicals were used to prepare the majority of the raw materials that were UV-cured in prior years. However, the depletion of petrochemical reserves and their detrimental environmental ramifications have underscored the necessity for alternative approaches. For this reason, there has been a recent surge in utilizing vegetable oils in UV-cured coatings. This shift is driven by the renewable nature of vegetable oils, their low toxicity profile, high applicability, and the seamless conversion of triglyceride structures into integral components of the coating matrix. In this study, Linseed oil, which is an environmentally friendly vegetable oil and has a higher rectivity than other oils, was used in the coating. First, the epoxidation process bonded functional groups of epoxy to linseed oil. Following this modification, the epoxy groups subjected to acrylation via a ring-opening reaction with acrylic acid (AELO). Additionally, a functional monomer that includes both thiol and carboxylic acid groups have synthesized utilizing 1,6-hexanedithiol and maleic anhydride to provide dynamic covalent bonds to the vegetable oil-based thiol-ene coating. Vegetable oil acrylates produced from linseed oil were combined with synthesized thiol and by adding different amounts of pentaerythritol tetrakis (3-mercaptopropionate) and cross-linked using UV light. The UV induced bio-based films and coatings obtained by thiol-ene click chemistry were then kept in a drying-oven at 120 °C for 1 hour and 24 hours with postcure application. Finally, the chemical, mechanical, thermal and surface properties of each films were examined. At the same time, coating performance tests carried out.

March, 2024 **Eda GAŞ**

SYMBOLS

g	**:** Gram
mg	**:** Milligram
°C	**:** Celsius
%	**:** Percentage
ml	**:** Mililitre
rpm	**:** Revolutions per minute
cm-1	**:** Wavelength
ppm	**:** Parts per million
h	**:** Hour
C	**:** Carbon
=	**:** Double bond structure

ABBREVIATIONS

TPP : Triphenyl Phosphine

VOCs : Volatile Organic Chemicals

VOBP : Vegetable oil-based polymer

CAGR : Compound Annual Growth Rate

AEO : Acrylated Epoxidized Oils

AEVOs : Acrylated Epoxidized Vegetable Oils

EVOs : Epoxidized Vegetable Oils

ESO : Epoxidized Soybean Oil

ALO : Acrylated Prepolymers

TEA : Triethylamine

LO : Linseed oil

AESO : Acrylation Epoxidized Soybean Oil

Tg : Glass Transition Temperature

PVC : Polyvinyl Chloride

TMPTA : Trimethylolpropane Triacrylate

DSC : Differential Scanning Calorimetry

FT-IR : Fourier Dönüşümlü Infrared Spektroskopisi

NMR : Nükleer Manyetik Rezonans

UV : Ultraviyole

LBEA : Lignin-based epoxy acrylate

PUA : Polyurethane acrylate

ACSO : Soy-based UV-curable branched oligomer

CNL : Cashew nutshell liquid

ESBO : Backbone of epoxidized soybean oil

CuAAC : Cu(I)-catalyzed azide–alkyne cycloaddition

DMAP : 4-Dimethylaminopyridine

H_2O_2 : Hydrogen peroxide

NMR : Nuclear magnetic resonance

PETMP : Pentaerythritoltetrakis(3-mercaptopropionate)

LIST OF FIGURES

PAGE

Figure 1.1. Triglyceride structure of the vegetable oil. 4

Figure 1.2. The chemical structure of the most common fatty acids. 4

Figure 1.3. Linseed oil market in the next year 8

Figure 1.4. Chemically reactive sites of a triglyceride molecule and potential reactions at each active site 9

Figure 1.5. The life cycle of a polymeric material derived from vegetable oil. 10

Figure 1.6. The schematic molecular structure of acrylated epoxidized triglycerides. 12

Figure 1.7. Synthesis of acrylated epoxidized soybean oil. 13

Figure 1.8. UV Curable Coating Process. 16

Figure 1.9. Structure of main acrylate reactive diluents. 18

Figure 1.10. The main types of acrylate resins and their schematic chemical structures for acrylate-based radically curing UV coatings. 20

Figure 1.11. Schematic representation of click chemistry reactions. 23

Figure 1.12. General radical thiol-ene reaction mechanism 26

Figure 1.13. A. The unexpected concentration-dependent inversion of the thiol-anhydride reaction in a polar environment, as corroborated by 1H-NMR evidence; B. suggested potential mechanisms for the reversible addition of thiols to anhydrides, either through thiol-thioester exchange (1) or reversible anhydride ring closure (2) 28

Figure 3.1. Acrylation of epoxidized linseed oil 37

Figure 3.2. Synthesis scheme of thiol compounds 38

Figure 3.3. Chemical structure of UV curable F1 formulation film with thiol-ene click chemistry 40

Figure 3.4. Chemical structure of UV curable F2 and F3 formulation film with thiol-ene click chemistry 41

Figure 4.1. FTIR analysis of epoxidized LO and linseed oil 43

Figure 4.2. FTIR spectra of acrylization of ELO 44

Figure 4.3. ^{1}HNMR spectra of acrylated epoxidized linseed oil 45

Figure 4.4. FTIR spectra of thiol compound 46
Figure 4.5. ^{1}HNMR spectra of thiol compound 47
Figure 4.6. FTIR Spectra of F1 Formulation Films 48
Figure 4.7. DSC analysis results of prepared F3 formulations 50
Figure 4.8. TG-DTA thermogram of prepared films 52
Figure 4.9. Images of coatings water contact angle 56
Figure 4.10. Adhesion test images of coatings 56
Figure 4.11. Scoring of cross-cut test results 57

LIST OF TABLES

PAGE

Table 1.1. Classification of vegetable oil 3
Table 1.2. Properties and fatty acid compositions of the most common vegetable oils . 6
Table 1.3. Some the physical and chemical characteristics of vegetable oils 6
Table 1.4. System components hardened by UV rays and their percentages in the formulation 17
Table 3.1. Raw materials used in the synthesis of epoxidized linseed oil 36
Table 3.2. Raw materials used in the synthesis of AELO 37
Table 3.3. Raw materials used in the synthesis of thiol compounds..... 38
Table 3.4. Formulations of UV cured films..... 39
Table 4.1. DSC analysis results of prepared films 49
Table 4.2. TGA analysis evaluation of prepared films 51
Table 4.3. Gel content analysis of the film in different formulations at different thermal times 53
Table 4.4. Tensile test analysis of prepared film 54
Table 4.5. Hardness test analysis of coatigs were prepared on microglass 54
Table 4.6. Hardness test analysis of coatigs on microglass..... 55
Table 4.7. Water contact angle values of coatings..... 55

1. GENERAL INFORMATION

Vegetable oils are types of oils that can be obtained from vegetable sources and consist of glycerides of fatty acids. This type of oil, which entered our lives with agriculture, has many uses in many fields. It was first used by people in the field of food and medicine. These ingredients, which also have great nutritional benefits for health, have been also used in therapeutic medicine over time.

In these days, the usage areas of these oils are expanding more and more. Vegetable oils are regarded as one of the foremost renewable resources due to they are easily derived from plants, their biodegradability, low cost, and low toxicity. Vegetable oils be utilized as a dependable beginning material to create new products with a variety of structural and functional modifications because they are acceptable the most important renewable raw material processed in the preparation of bio-based functional polymers and polymeric materials [1].

For instance, they can produce monomers with similar structures to petroleum-based monomers and they serve as building blocks for the monomer chains needed to create a variety of polymers including polyester polyurethane, polyolefin, and polyether. Thus, the vegetable oil-based polymer (VOBP) structures can be easily modified. The recent increase in the use of renewable resources as a replacement for products based on fossil fuels is due to the need to reduce the carbon footprint, which is one of the environmental concerns, apart from the financial constraint of oil. Plants achieve a neutral carbon footprint by using atmospheric carbon as CO_2 to produce oils and then they are subsequently transformed into composites and polymers. Examples of plant-derived oils used to make a range of polymers include soybean, palm, linseed and sunflower oils. Polymers derived from vegetable oil are used in many fields such as paints, adhesives coatings, and biomedicine. Thus, the aim is to offer more environmentally friendly and less biohazardous products [2, 3, 4].

Today, vegetable oils have roles in numerous industries in addition to being used as ingredients in food. Vegetable oil consumption has been projected to be 219 million tons in 2020, and 285 million tons are anticipated to be consumed in 2026. The worldwide vegetable oil market, which was valued at 215.4 million metric tons in 2022, is projected

to grow to 315.1 million metric tons by 2030. This growth represents a compound annual growth rate (CAGR) of 4.9% from 2022 to 2030, following adjustments for the post–COVID–19 market landscape [5].

1.1. Extraction and Classification of Vegetable Oil

In the production of vegetable oils, the oil must initially be extracted from the oil-containing parts of plants, which are frequently seeds. This situation can be achieved either through mechanical extraction using a chemical extraction or an oil mill employing a solvent. The obtained oil can then be cleansed, purified, or subjected to chemical alterations as necessary. In commercial applications, vegetable oil is typically extracted utilizing solvent extracts, which generate larger yields and is faster and less expensive. Various mechanical pressing methods, solvent extraction techniques, or a blend of both are employed to derive vegetable oils from seeds, fruits, or nuts rich in oil. The crude oils extracted undergo refinement through a series of physical and chemical treatments. Vegetable oils are derived from a range of origins. These include popular vegetable oils such as cottonseed, sunflower oils, peanut, and soybean, as well as linseed oil, palm oil, rapeseed oil, castor oil, coconut oil and others [16].

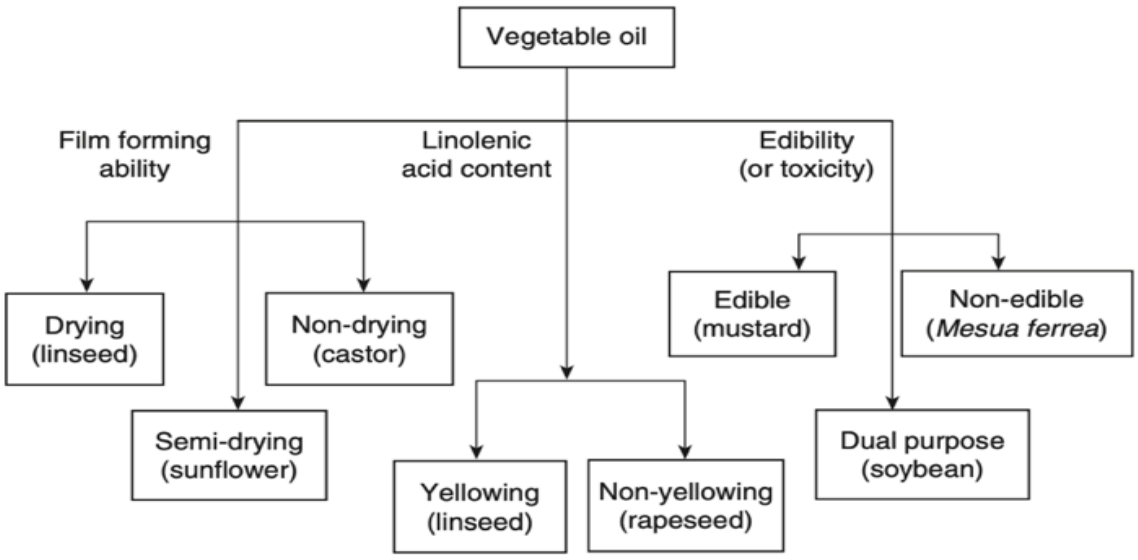
There are two different fatty acid triglycerides in nature, simple triglycerides and mixed triglycerides. Fatty acids containing triglycerides in a single ratio are called simple triglycerides, fatty acids containing triglycerides in different ratios are called mixed triglycerides. When the structure of vegetable oils in nature is examined, all oils are in the mixed triglyceride class except jojoba oil, which is called simple triglyceride [6].

It enables them to have different physical and chemical properties due to the difference in the amount and location of the double bonds within the fatty acid chain**.** Fatty acids that have at least one double bond are known as unsaturated fatty acids, whereas those without any double bonds are called saturated fatty acids. The degree of unsaturation is enunciable as a measure of iodine value. Vegetable oils are divided into 3 groups according to existence of double bonds the degree of unsaturation and the structure of the fatty acid. These are non-drying, drying and semi-drying oil. [6, 7].

The iodine value (IV) used to classify vegetable oils is a parameter that measures the degree of unsaturation per 100 g of sample by means of titration or ^{1}H NMR. A larger IV

value indicates a higher the level of unsaturation in each triglyceride of vegetable oil. Value IV > 130 for oils drying in the parameters indicated by IV values; for semi-drying oils 100 < IV < 130; for non-drying oils, it has IV < 100. When classifying vegetable oils, they are categorized as yellowing or non-yellowing according to their linolenic acid content. Drying oils typically turn yellow, although semi-drying and non-drying oils don't turn yellow. The iodine value of vegetable oil might vary depending on the type and age of the plant, and the extraction process. In addition, the high degree of unsaturation of the fatty acid indicates that it is more sensitive to chemical modification [6, 8, 9]. The Table 1.1 below shows the classification of vegetable oils.

Table 1.1. Classification of vegetable oil [6].



1.2. Structure and Properties of Vegetable Oil

The primary ingredients of vegetable oils include triglycerides, which are formed by transforming glycerol with three fatty acids and comprise carbon, hydrogen, and oxygen in their structure (Figure 1). According to the kind of plant and the climatic circumstances in which it is grown, vegetable oils are also known as glycerin and esters of wide range of fatty acids comprising between 8 and 24 carbon atoms with 0 to 7 carbon-carbon double bonds [1, 10]. Fatty acids make up 95% of the oil triglyceride molecule's total weight and their amounts differ depending on the plant oil. Triglycerides represent the same or different fatty acids, as well as multiple reactive sites for instance ester groups,

double bonds**,** which gives up more potential for structure modification. [11, 12]. The triglyceride structure of vegetable oil is shown in Figure 1.1 below.

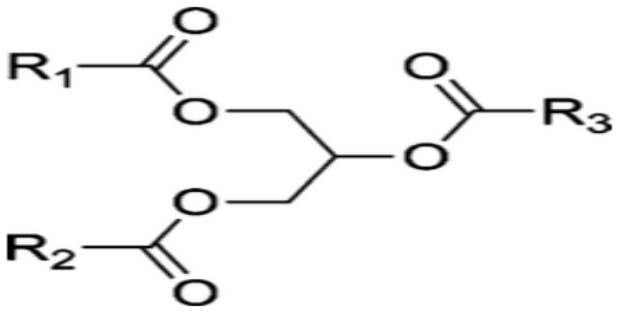


Figure 1.1. Triglyceride structure of the vegetable oil [17].

The application areas of vegetable oils differ according to the fatty acids contained in them. This distinction between the properties of fatty acids is determined by the growing conditions, the chain lengths they have, the number and position of C=C bonds, the degree of unsaturation regions, and the presence of functional groups (for example, hydroxyl and epoxy) [4, 18]. The majority of fatty acids are made up of straight-chain molecules with an even number of carbon atoms ranging from 8 to 24, with 16, 18, 20 carbon atoms being the most common. Examples of fatty acids that make up the basic composition of vegetable oils are linoleic, oleic, stearic, palmitic and linolenic fatty acids [4, 14, 15]. The chemical structures of the most common fatty acids found in vegetable oils are given in Figure 1.2.

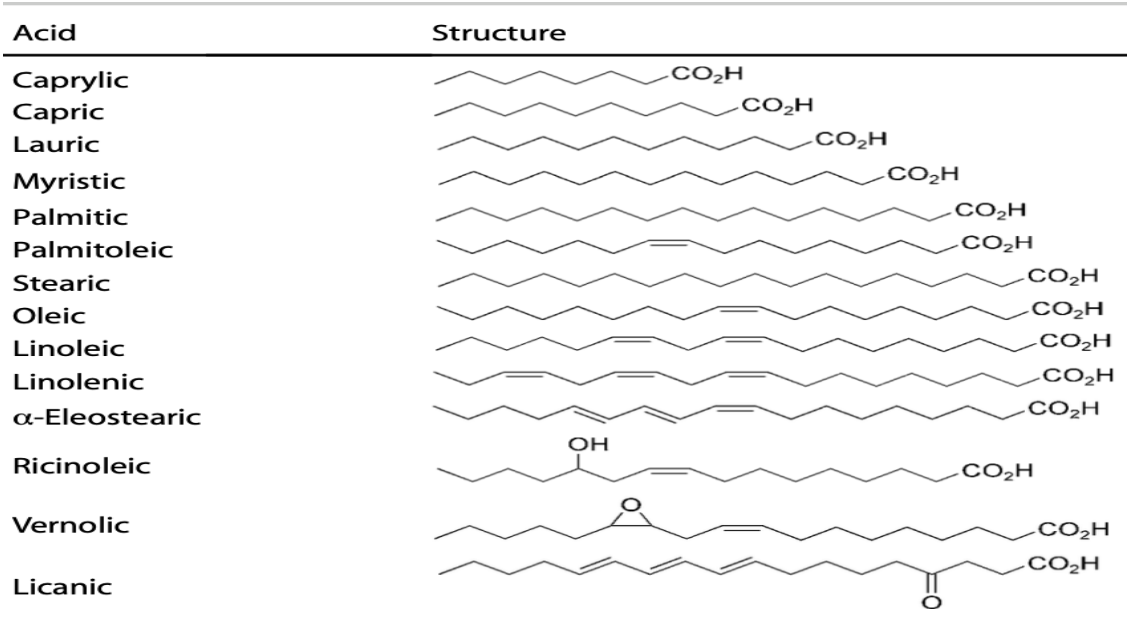


Figure 1.2. The chemical structure of the most common fatty acids [15].

Fatty acids can be saturated, unsaturated, conjugated, or isolated according to their different structural properties. There aren't double bonds in saturated fatty acids. However, some unsaturated fatty acids can be polyunsaturated structures containing more than two C=C double bonds or monounsaturated containing one C=C double bond [14]. While oleic acid is given as a fatty acid example that is monounsaturated, fatty acids such as linoleic and linolenic can be given as examples of fatty acids with polyunsaturated structure. In addition, some saturated fatty acids can be listed as palmitic, lauric, lignoceric and behenic. When the fatty acids in the structure of most vegetable oils were examined, it was observed that the double bonds of fatty acids such as linoleic acid and oleic acid were in the cis configuration. However, small amounts of trans isomers can also occur, as for example in α-eleostearic and licanic acids [16]. Among the most significant elements influencing the chemical and physical properties of vegetable oils is the degree of unsaturation of fatty acids, and the unsaturation bond content can be measurement of the iodine value (IV) allows for determination. The IV value is the quantity of iodine (mg) in 100 g of vegetable oil that reacts with the carbon-carbon double bonds [17]. Since the double bond content is directly related to the iodine value, a high iodine value means that the level of unsaturation is high, that is, the fatty acid chain has a high level of carbon-carbon double bonds. For instance, linolenic acid in linseed oil; soybean oil is dominated by linoleic acid. When we compare two vegetable oils, three carbon-carbon double bonds in the chain of Linolenic acid indicates that it has more reactive sites. This means that linseed oil with three carbon-carbon double bonds will be more easily modified than soybean oil with two carbon-carbon double bonds [12, 14].

When carbon atoms alternate between single and double bonds, the double bonds are referred to as conjugated [11]. Most vegetable oils include Carbon-carbon double bonds that naturally form between the 9th and 16th carbon atoms. Due to the presence of allylic hydrogens within the methylene group that is positioned between double bonds, the majority of naturally occurring carbon-carbon double bonds are non-conjugated, hence less reactive [12]. When we examine the structural properties of fatty acids, in addition to the examples given above, some fatty acid chains include functional groups such as epoxy, hydroxy or oxo groups in the proximity of double bonds. Each fatty acid has different physical properties due to structural variations [11, 13, 15]. The composition of fatty acids in vegetable oils varies based on the cultivation conditions of the source plant,

the time of year, the carbon chain length of the fatty acids, stereochemistry of the double bonds, and the level of unsaturation. A detailed breakdown of the fatty acid content in the most commonly used vegetable oils can be found in Table 1.2. [12, 16, 17].

Table 1.2. Properties and fatty acid compositions of the most common vegetable oils [17].

			Fatty acids (%)				
Vegetable oil	**Double bonds**	**Lodine value/mg per 100 g**	**Palmitic**	**Stearic**	**Oleic**	**Linoleic**	**Linolenic**
Palm	1.7	44-58	42.8	4.2	40.5	10.1	-
Olive	2.8	75-94	13.7	2.5	71.1	10.0	0.6
Groundnut	3.4	80-106	11.4	2.4	48.3	31.9	-
Rapeseed	3.8	94-120	4.0	2.0	56.0	26.0	10.0
Sesame	3.9	103-116	9.0	6.0	41.0	43.0	1.0
Cottonseed	3.9	90-119	21.6	2.6	18.6	54.4	0.7
Corn	4.5	102-130	10.9	2.0	25.4	59.6	1.2
Soybean	4.6	117-143	11.0	4.0	23.4	53.3	7.8
Sunflower	4.7	110-143	5.2	2.7	37.2	53.8	1.0
Linseed	6.6	168-204	5.5	3.5	19.1	15.3	56.6

While the majority of vegetable oils remain in a liquid state at ambient temperature, it is important to note that this is not the case for all vegetable oils [17]. Because they include aliphatic hydrocarbon chains, triglycerides are insoluble in water but soluble in solvents such as hexane and acetone. Vegetable oils lacking any functional groups aside from their ester moieties exhibit Newtonian fluid behavior with low viscosity. However, when unsaturation in the aliphatic chains and other functionalities such as carbonyl groups, epoxy, or hydroxyl, are present, the viscosity of the oils may experience a notable increase. The type of constituent triglycerides influences the melting behavior of vegetable oils. Thus, triglycerides mostly made of long-chain saturated acids possess elevated melting temperatures, whereas those primarily composed of polyunsaturated acids have lower melting points. [16]. Table 1.3 below presents the physicochemical properties of certain vegetable oils

Table 1.3. Some the physical and chemical characteristics of vegetable oils [16].

Name	**Kinematic viscosity (cSt at 37.8 ^{0}C)**	**Specific gravity (20 ^{0}C/4 ^{0}C)**	**Refractive index (n_D ^{20})**	**Melting point / (^{0}C)**
Castor oil	293.4	0.951-0.966	1.473-1.480	-20 to -10
Linseed oil	29.60	0.925-0.932	1.480-1.483	-20
Palm oil	30.92	0.890-0.893	1.453-1.456	33 to 40
Soybean oil	28.49	0.917-0.924	1.473-1.477	-23 to -20
Sunflower oil	33.31	0.916-0.923	1.475-1.477	-18 to -16

1.2.1. Linseed oil

The Latin botanical name for flaxseed is Linum usitatissimum, translating to “very useful.” [19]. Linseed, also known as flax, is predominantly cultivated in warm temperate zones or subtropical regions. The leading producers of linseed include Argentina, the Canada, United States, India and Russia [20]. It contains the greatest number of double bonds compared to all other vegetable oils, and the presence of unsaturated C=C double bonds in its molecular structure endows it with substantial chemical reactivity. Significantly, a range of modification reactions can be applied to the reactive sites such as C=C double bonds, propylene carbons and ester groups, along the carbon chain of linseed oil. These modifications could establish functional groups with enhanced polymerization capability, thereby enhancing its functionality and the extent of conjugation [21]. Traditionally, it has been employed as a foundational component for paint, ink, and coating agents owing to its capability to undergo autoxidation, allowing it to dry in the presence of atmospheric oxygen [22]. Linseed oil has also been used in the production of thermosetting polymers and composites, where its high content of linolenic acid allows it to react with atmospheric oxygen and form a three-dimensional network. gen [23]. Linseed oil is recognized as a nutritious oil because of its abundance of omega-3 fatty acids and other advantageous compounds. It is utilized as both a dietary supplement and as an ingredient in functional foods [24].

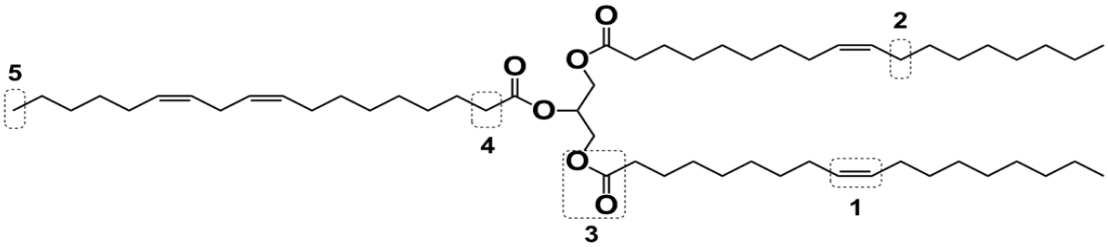
The Linseed Oil Market exceeded USD 2.85 billion in 2021 and is projected to expand with a CAGR of over 5.5% between 2021 and 2028. Growing attention from cultivators towards integrating linseed oil in conventional agricultural practices, driven by increasing consumer awareness of nutrition, is expected to boost the product's demand. Linseed oil boasts rich nutritional elements, encompassing fats, omega fatty acids, and other essential constituents. Its application spans across diverse industries including paint and varnishes, cosmetics, food, animal nutrition, and pharmaceuticals [25]. The Figure 1.3 below shows the projected consumption of flaxseed in the next year.



Figure 1.3. Linseed oil market in the next year [25].

1.3. Chemical Modification of Vegetable Oil

Vegetable oils are regarded as renewable resources due to their adaptability to chemical modification, low cost, ease of availability, and biodegradability, and are seen as a potential alternative to polymers made from fossil fuels. Since vegetable oils have weak chemical reactivity. Vegetable oils can't therefore be easily transformed into polymers without adding more reactive functions to their molecules, including vinyl, epoxy, or hydroxyl groups [26]. Unsaturated fatty acids, their alkyl esters, and triglycerides of vegetable oils all have active sites that can be functionalized and employed for polymerization with the right procedures [27]. Thus, the double bonds **w**ithin the oil chain to procedures including epoxidation, acrylation, thiol-ene coupling, maleinization, and hydroxylation, renewable monomers can be created from oils by subjecting [9]. Figure 1.4 below includes the ester groups, double bonds, allylic carbons, and a-carboxylic carbons of triglyceride molecules, and this scheme includes information about which reactions occur to modify the triglyceride [16].



(1) double bond	(2) allylic carbon	(3) ester group
- oxidation	- halogenation	- hydrolysis
- epoxidation	- hydroperoxidation	- alcoholysis
- hydroformylation	- hydroxylation	- transesterification
- dimerization	- electrochemical acetylation	- saponification
- ozonolysis		- halogenation
- metathesis	**(4) α-carbon**	- reduction
- thiol-ene coupling	- α-sulfonation	- amidation
- hydrogenation	- α-halogenation	
- pericyclic reaction	- alkylation	**(5) ω-carbon**
- sulfonation	- acylation	- ω-oxidation
- carbonylation	- Claisen condensation	

Figure 1.4. Chemically reactive sites of a triglyceride molecule and potential reactions at each active site [16].

Modification of the double bonds enables the addition of functionalities such as maleates, hydroxyl, or epoxy groups, thereby allowing subsequent reactions through polycondensation polymerization or ring-opening Following this reaction stage, the resulting product can be utilized directly in crosslinking reactions without additional modifications, or it can undergo further chemical processes, expanding the range of functional molecules that can be obtained [28]. The fundamental idea of chemical modification is to achieve an elevated molecular weight and increased crosslinking density, both recognized as pivotal factors significantly affecting the stiffness within the polymer network. Additionally, it aims to introduce chemical functionalities recognized for enhancing stiffness within a polymer network, such as aromatic or cyclic structures [29]. Figure 1.5 below shows the life cycle of polymers derived from vegetable oils and the extraction of biomass from plant-based sources to obtain vegetable oil [28].

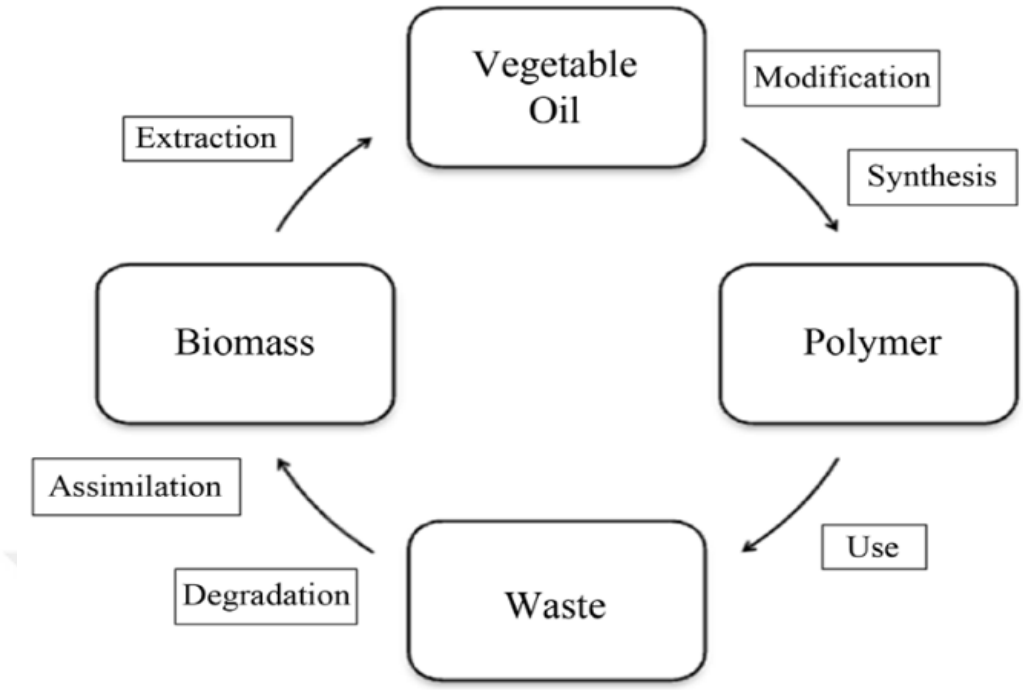


Figure 1.5. The life cycle of a polymeric material derived from vegetable oil [28].

1.3.1. Epoxidation of vegetable oil

Epoxidation in vegetable oils involves adding an oxygen atom to the double bonds within the fatty acid chains of triglyceride molecules, resulting in the formation of a cyclic ether structure. These epoxidized oils, being biodegradable, non-toxic, and naturally derived, present promising alternatives to chemicals derived from petroleum [30]. The epoxidation process holds significance in organic synthesis due to the formation of epoxides, which serve as crucial intermediates convertible into a diverse range of products [31]. Due to the high reactivity of the oxirane ring, epoxides are considered important basic materials in synthesizing a wide array of chemicals, including alcohols, glycols, olefinic compounds, lubricants, plasticizers, and polymer stabilizers. The demand for these compounds is consistently on the rise. Converting vegetable oil into epoxidized vegetable oil has the potential to elevate its economic value. The double bonds present in the vegetable oil act as reactive sites in coatings and can be functionalization via epoxidation. This process enables the production of high molecular-weight products by intensifying the cross-linking [32].

Various techniques can be employed to achieve the epoxidation of vegetable oils. Examples of epoxidation methods include conventional epoxidation, enzyme-mediated epoxidation, metal-catalyzed epoxidation, and acid ion exchange epoxidation [32]. The process of epoxidation involves the reaction between the oil and an epoxidizing agent like hydrogen peroxide (H_2O_2), typically in the presence of a catalyst such as formic acid or sulfuric acid [33].

Linseed oil has the highest unsaturated C=C double bond content among vegetable oils, giving it an advantage in terms of chemical reactivity. Rosa and et al. conducted a study to determine the influence of linseed oil's high unsaturation on the selectivity and reactivity of the epoxidation reaction**.** Various kinetic experiments involving the epoxidation of linseed oil using performic acid generated in situ and phosphoric acid as a catalyst have been conducted. These experiments were analyzed using a biphasic kinetic model previously employed in soybean oil epoxidation. As a result of the experiment is showed linseed oil has shown approximately 1.5 times greater reactivity compared to soybean oil, owing to the higher level of unsaturation present in the molecules of linseed oil. The oxirane ring-opening reaction reveals that the reactivity of epoxidized linseed oil is a minimum of four times greater than that of soybean oil. This heightened reactivity is likely attributed to the mutual inductive effects facilitated by the neighboring oxirane groups [34]. In other study, Resch-Fauster and et al. focused on improvement a pliant epoxy resin containing 100% bio-based carbon content. Linseed oil, Soybean oil and hemp oil were epoxidized. The mechanical properties of epoxy resins derived from epoxidized vegetable oils have also been investigated, and it has been shown that these resins possess good mechanical strength and flexibility. When comparing the performance of vegetable oils, it was concluded that using epoxidized linseed oil resulted in attaining the highest Tg (glass transition temperature) and optimal mechanical properties, including the highest tensile strength and toughness [35].

Epoxidized vegetable oils serve as intermediates for a wide array of applications. They are utilized as plasticizers and stabilizers in polymers, components in plastics additives in lubricants, and in the form of polyols for producing urethane foams [36]. Epoxidized vegetable oils find significant application as plasticizers in polyvinyl chloride (PVC) formulations. They serve as successful alternatives to conventional phthalate-based plasticizers, providing enhanced compatibility and thermal stability [37]. Furthermore,

these oils have been used as processing aids and activators in rubber compounds, enhancing the processability and mechanical properties of the rubber [38]. Moreover, beyond their conventional role as plasticizers and processing aids, epoxidized vegetable oils have undergone exploration as potential raw materials in polyol synthesis. Polyols derived from these oils display promise as sustainable and renewable alternatives to petroleum-derived polyols in the manufacturing of polyurethane foams [39]. Overall, epoxidized vegetable oils offer a wide range of potential applications in numerous industries, including plastics, rubber, and polyurethane production.

1.3.2. Acrylation of vegetable oil

Acrylated epoxidized oils (AEO) can be readily produced by subjecting epoxides to a ring-opening reaction with acrylic acid This reaction produces acrylate functionalities on the aliphatic chain with a vicinal hydroxyl group [40]. The acrylation process is employed to chemically enhance EVOs, creating more value-added products. Bio-based polymers and resins derived from these AEVOs are gaining significant attention in both research and industrial applications due to their numerous advantages over conventional petroleum-based polymers. These biopolymers are not only biodegradable, renewable resources but also more cost-effective as raw materials. In addition to their potential to replace petroleum-based polymers, AEVOs can undergo UV curing for further improvement of their properties in the curing and coating industries [41].

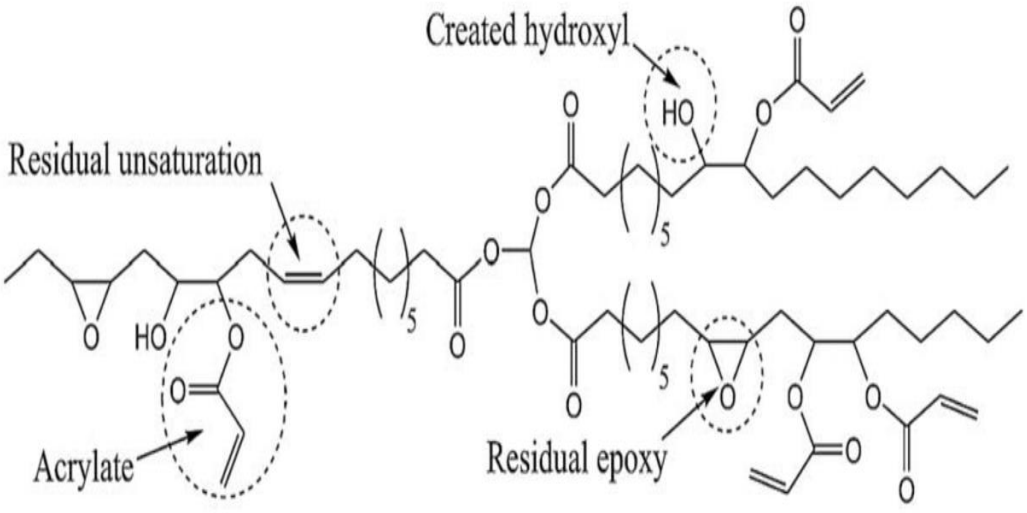


Figure 1.6. The schematic molecular structure of acrylated epoxidized triglycerides [42].

Habib et al. investigated the curing process of biodegradable polymer films made from soybean oil through ultraviolet light exposure and evaluated their thermal degradation resistance. Moreover, an epoxy acrylate resin was synthesized from epoxidized soybean oil (ESO) by employing an acrylic acid monomer. Triethylamine (TEA) was used as the catalyst, while hydroquinone functioned as the inhibiting agent. The acrylation of epoxidized soybean oil (AESO) involved the introduction of acrylic acid, an unsaturated monomer, into the oxirane groups of the epoxidized oil (ESO). Various formulations for UV curing have been studied, incorporating a synthesized acrylated resin and a trifunctional acrylate monomer as cross-linkable active diluents, with a photoinitiator. Upon the addition of the photoinitiator and reactive diluent, the resin became capable of UV curing. UV-cured films demonstrate favorable thermal stability, characterized by a decomposition rate of approximately 473 K. Figure 1.7 below shows the diagram of epoxidized acrylated soybean oil [43].

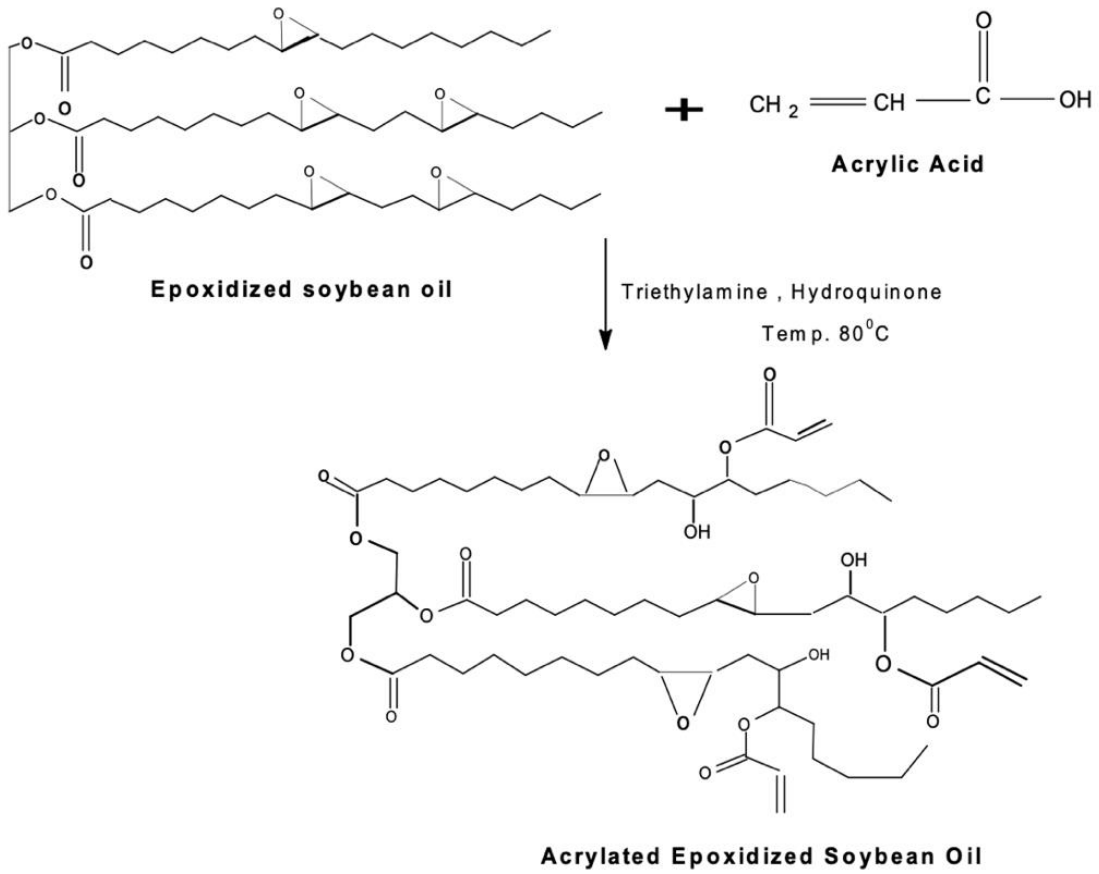


Figure 1.7. Synthesis of acrylated epoxidized soybean oil [43].

Grishchuk et al. focused on the modification of soybean oil and linseed oil with epoxy, the preparation and comparison of acrylated linseed and soybean oil (AESO and AELO) derivatives, and the differences in epoxy grades resulting from different unsaturated fatty acid contents in triglyceride structures. Accordingly, it has been reported that each of them is acrylated at different rates [42]. In another study conducted, Su et al. employed an innovative single-step approach to synthesize 2.5-functional acrylated prepolymers (ALO) derived from linseed oil. The process involved the utilization of linseed oil and acrylic acid as the primary substances, with boron trifluoride diethyl ether acting as the catalyzing agent. Moreover, various types of UV-curable films were formulated by blending ALO with polyurethane acrylate resin, photoinitiator and trimethylolpropane triacrylate (TMPTA). The study revealed that increasing the crosslinking density had positive effects on various properties of the cured films, such as dynamic mechanical properties, thermal stability, and mechanical properties. Notably, the cured films exhibited adhesion, excellent hardness, and resistance to water/solvents. The research proposes a straightforward method for producing UV-curable acrylated prepolymers from linseed oil. Given the economic and renewable nature of linseed oil and the impressive performance of the cured films, ALO emerges as a biodegradable, sustainable substance for coatings that resist corrosion [21]. The use of acrylated vegetable oils in various applications has also been explored. For example, Briede et al. (2022) investigated the use of UV-assisted 3D printing for the production of photoactive vegetable oil acrylates. They discussed the two common methods employed to acquire acrylated vegetable oils including the ring-opening reaction of epoxides and the direct single-step addition employing catalysts. This study demonstrates the potential of acrylated vegetable oils in the field of additive manufacturing [44].

1.4. Coatings Prepared by UV Curing

For years, it has been recognized that volatile organic compounds (VOCs) in the atmosphere not only contribute to severe air pollution problems due to their toxic or carcinogenic properties but also indirectly contribute to global warming. In addition to the current challenges faced by the coating industry in regulating VOCs, there is a growing concern about energy consumption, particularly the use of fossil-fuel resources. This is because the polymer and coatings sectors heavily rely on petrochemical products

derived from crude oil, which are expected to become scarce in the future. A potential solution to address both the VOC restriction and energy consumption issues involves the adoption of advanced UV-curable systems. These systems are characterized by being solvent-free and having low energy consumption, presenting a high-tech approach to mitigating environmental challenges [45]. UV-curable coatings, offering low VOC emissions, rapid curing, and energy efficiency, hold significant promise as an alternative to traditional solvent-borne coatings [46]. The UV-curing industry, commercially introduced in the 1970s, has experienced consistent growth and emerged as one of the most rapidly advancing sectors in the coatings industry. UV-curable coatings, valued for their high curing efficiency and minimal VOC emissions, have widespread applications in surface protection across various materials like metals, plastics, wood, paper, 3D printing, glass, food packaging, electronic devices, etc [45, 47]. Vegetable oils, serving as a significant source of bio-based chemicals, emerge as prominent candidates for replacing fossil feedstock. Their attributes of biodegradability, abundance, and relatively low-cost position them favorably and is used in diverse fields, including inks, elastomers, coatings, and adhesives [48].

UV-curable materials primarily consist of composites derived from raw materials derived from petroleum such as photoinitiators, prepolymers, and reactive diluents**.** In response to the global energy crisis and environmental concerns arising from the exhaustion of fossil resources and petrochemical industry pollution, considerable efforts have been directed toward replacing petroleum-based materials with renewable alternatives in UV-curable material development. Plant oils, recognized as significant renewable resources, have emerged as a preferred choice for creating UV-curable materials. Their distinct advantages, including low viscosity, low toxicity at room temperature, low cost, high availability, ease of modification, unique triglyceride structure, contribute to their preference in this application [49]. Utilizing bio-based sources like annually renewable vegetable oils offers a strong alternative foundation for developing advanced sustainable materials. By employing chemical transformations, it becomes feasible to produce bio-based materials that not only have a substantially reduced carbon footprint but also meet the high-performance requirements of their respective products [50]. UV ray-prepared coating formulations consist of various components such as oligomers (for film formation and essential properties), photoinitiators, reactive diluents (for cross-linking), fillers, and

additives. Applied as a liquid with viscosity variations determined by the oligomer type and reactive diluent, the coating undergoes exposure to UV rays of suitable wavelength and energy after application to the surface. The hardening process takes place through either a free radical or cationic mechanism. The completely hardenered coating exhibits a high molecular weight, cross-linked, and non-adhesive configuration. All reactive components within UV-curable systems undergo reactions and contribute to the polymer's network structure, meaning that 100% of the applied coating hardens without leaving any residue on the surface. These coatings are recognized as environmentally friendly as they do not release volatile components during the hardening process [51]. UV-curable formulations are comprised of photosensitive organic groups featuring unsaturated carbon double bonds (C=C) that can undergo polymerization upon exposure to UV radiation. All photochemical reactions depend on activating excited molecules with specific energy, structure, and lifetime. Photoinitiators are distinguished by the existence of at least one aromatic rings with a carbonyl (C=O) group in their structure, and they exhibit strong absorption of UV radiation. The absorption of light energy by the photoinitiator leads to the formation of excited molecules [52].

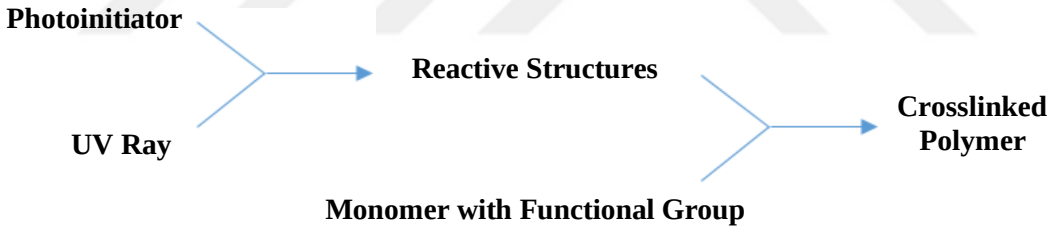


Figure 1.8. UV Curable Coating Process [52].

Photoinitiators absorb UV rays in the 200–400 nm wavelength range, transferring substantial reactive chemical energy to radicals. These radicals then break the double bonds in the oligomer and monomer mixture, initiating a chain reaction. The polymerization of oligomers and monomers forms a network through the chain reaction. As the molecules grow, their flexibility diminishes, leading to the eventual cessation of the chain reaction. The coating has transformated from liquid to solid [52].

1.4.1. UV-curable system components

Protective coating formulations prepared with UV rays typically consist of three main elements:

- Reactive Oligomers
- Reactive solvents
- Photoinitiators

Table 1.4. System components hardened by UV rays and their percentages in the formulation [53].

Components	Percent By Mass	Function in Formulation
Photoinitiator	1-3	Free radical or cationic initiator
Reagent diluent	15-60	Film formation and viscosity control
Reaktif oligomerler	25-90	Film formation and basic properties
Additives and filling materials	1-50	Surfactants, pigments
Source of Light	-	Energy requirement

Additionally, a diverse range of chemical structures is employed as additives for various purposes, including reactive filling pigments, structures enhancing adhesion, softeners, structures regulating fluidity, paints, and surface lubrication structures [53].

1.4.1.1. Photoinitiators

Photoinitiators generate free radicals upon exposure to UV light, initiating the crosslinking polymerization of the resin system [54]. Oligomers and monomers typically do not absorb adequate light within the UV range of 200-400 nm. Therefore, UV-sensitive initiators, also known as photoinitiators, are incorporated to initiate photopolymerization [55]. Photoinitiators, typically added to the coating formulation at a rate of 1-3% by weight, can be categorized into eight classes. These classes include synergistic amines and aromatic ketones and alkyl benzoin ethers, thioxanes and benzyl ketals ,their derivatives, acylphosphine oxide, ketoxime ester or acyloxime esters, cationic dried quaternary ammonium salts, and acetophenone derivatives. The selection of the appropriate photoinitiator for the application should align with the absorption wavelength of the oligomers utilized in the formulation, its chemical composition, the type and positioning of the UV lamp, the curing rate, and the intended surface characteristics [56]. High concentrations of photoinitiators are employed only when significant oxygen inhibition effects are present. In inert conditions, a photo-initiator concentration of 0.5–1% is typically sufficient for curing. Using a higher concentration of photoinitiator often

results in an inner filter effect in the film, impeding light penetration to the lower layers and causing inadequate through-cure [55]. An efficient photoinitiator should possess the capability to absorb light across a broad emission spectrum ($248 < \lambda < 578$). When selecting a photoinitiator, it is crucial to verify its cost-effectiveness, resistance to yellowing, lack of odor, low volatility, non-toxicity of both the photoinitiator and its degradation products, strong absorption within the activation range, and easy solubility in resins [57].

1.4.1.2. Reactive solvents

Reactive diluents are incorporated to decrease viscosity and enhance the crosslink density of the system in a formulation for UV-curable coatings [55]. Reagent diluents have a substantial impact on various parameters, including curing speed, film properties, shrinkage during polymerization, odor, shelf life, toxicity, cost and volatility Acrylates stand out as the most commonly used reactive diluents in UV-curable systems due to their versatility and reactivity. Beyond their rapid curing rates compared to other monomer systems, acrylates are available in a diverse range of structures, including monofunctional, difunctional, trifunctional, and tetrafunctional varieties. General chemical structures of reactive diluents are given below figure 1.9 [45].

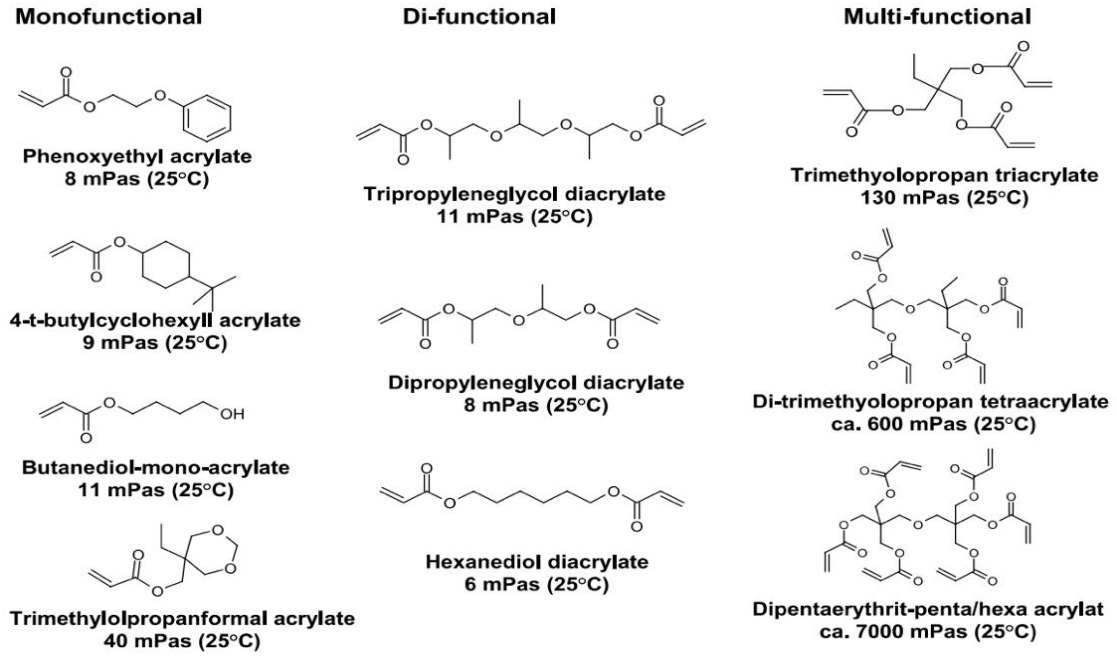


Figure 1.9. Structure of main acrylate reactive diluents [58].

Monofunctional acrylates are compounds with low film viscosity that are frequently employed as reactive diluents to reduce the viscosity of the coating. This is advantageous for the application of the coating and the process of film formation. Multifunctional acrylates are relatively low viscosity molecules used to increase the cure speed and cross-linking density due to their polyfunctionality [59]. Prepolymers, reactive diluents and prepolymers are essential components in forming a UV-curable system, traditionally sourced from petroleum-based substances. However, the growing interest in bio-based materials and renewable, such as lignin, cellulose and vegetable oils, offers a greener alternative. The development of vegetable oil-based raw materials represents a significant step toward environmentally friendly UV-curable coatings. Modifications at the reactive sites within the structure of vegetable oil,as suggested by Su et al., introduced an innovative approach for the synthesis of a multifunctional cardanol-based UV-curable reactive diluent (CACAA). This diluent, when applied in UV-curable coatings with a high bio-based content derived from cardanol derivative (CACAA) and soybean oil (AESO), outperformed petroleum-based diluents like BPAEODA and PETA. CACAA demonstrated the best dilution effect, striking a favorable equilibrium between augmenting mechanical and thermal attributes while reducing volume shrinkage in the cured films [60].

1.4.1.3. Reactive oligomers

UV-curable coatings present advantages over traditional coatings, offering higher curing efficiency, environmental friendliness, and reduced energy consumption. These systems typically consist of active diluents, photosensitive oligomers, additives and photoinitiators. Photosensitive oligomers, crucial in UV curing, include polyester acrylate, epoxy acrylate and polyurethane acrylate. Nevertheless, many conventional oligomers are derived from petroleum, expensive, and environmentally concerning. To address these issues, there is a growing demand for a cost-effective, readily available, renewable, and eco-friendly UV-curable oligomer. Recently, bio-based materials, including vegetable oils and proteins, have gained widespread usage in the coating industry. This trend is attributed to their renewable nature, environmental friendliness, and abundant availability [61].

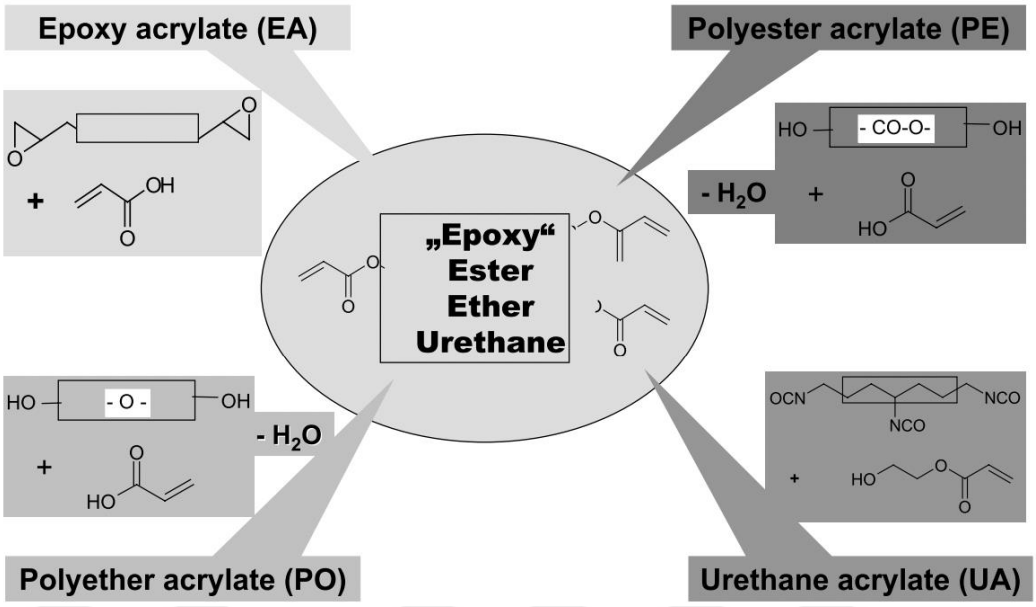


Figure 1.10. The main types of acrylate resins and their schematic chemical structures for acrylate-based radically curing UV coatings [58].

Although EA is widely used due to its low cost, quick curing time, and desirable coating properties, its high brittleness and poor flexibility on soft substrates pose challenges. To address these issues, a UV-curable epoxy acrylate oligomer with high flexibility and low viscosity, named bisphenol A epoxy acrylate (MHEA), was developed. This modification involved using a carboxyl-terminated intermediate to enhance the flexibility of the cured film, adjusting flexibility through the carbon chain length of diols. MHEA exhibited lower viscosity and excellent flexibility compared to commercially available modified EA and unmodified. The resulting cured film demonstrated adhesion high gloss,impact resistance, chemical resistance, impact resistance, and a pencil hardness of H, addressing the shortcomings associated with EA [62]. Epoxy acrylate (EA) resin, recognized for its exceptional properties including outstanding adhesion, chemical resistance flexibility, and hardness, is utilized as a resin for UV curing coatings. The production of epoxy acrylate involves the introduction of C=C double bonds and vinyl ester groups into epoxy resin, enabling its cure with radical photoinitiators. Despite its advantageous features, the application of EA resins is constrained by drawbacks, notably poor resistance to light aging. Yan et al. synthesized lignin-based epoxy acrylate (LBEA) oligomer with various percentages of lignin in situ using acrylic acid and epoxy. Therefore, which subsequently underwent UV curing to form membrane coatings**.** The addition of lignin significantly enhanced the mechanical properties and chemical resistance of the coatings compared to

epoxy acrylate (EA) resin. This finding demonstrates the promising potential of lignin as a novel biomaterial for the development of biobased epoxy acrylate (EA) coatings. [63].

Hu et al. have studied the utilization of bio-based materials in the coating industry, particularly focusing on the synthesis and characteristics of UV-curable multifunctional polyurethane acrylate resins derived from cardanol.In this study, a new polyfunctional polyurethane acrylate (PUA) oligomer based on cardanol was successfully synthesized through a straightforward two-step process. Furthermore, the UV-cured biomaterials, incorporating the HEMA diluent, displayed exceptional properties, including storage modulus, glass transition temperature (Tg), tensile strength maximum thermal degradation, temperature, and modulus, as well as flexibility of coatings and adhesion.These superior characteristics can be attributed to the high C═C functionality of the oligomer and the unique structures, such as the benzene ring, present in cardanol. As a result, the developed cardanol-based PUA resins was find to hold potential for applications in UV-curable materials, particularly coatings [64]. Another study introduces an eco-friendly strategy to enhance the performance and biorenewable content of UV-curable materials derived from natural plant oils. A new soy-based UV-curable branched oligomer (ACSO) was synthesized through the chemical integration of cashew nutshell liquid (CNL) into the backbone of epoxidized soybean oil (ESBO), succeeded by epoxidation and acrylation. In comparison to coatings derived from acrylated epoxidized soybean oil (AESO), ACSO-based coatings have been found to exhibited superior impact resistance, improved crosshatch adhesion, mechanical properties and enhanced thermal. This approach offers a promising direction for developing UV-curable bio-based oligomers containing a significant number of renewable resources [65].

1.4.2. Advantages and disadvantages of UV curable coatings

Advantages:

- Reactive diluents, capable of polymerizing with prepolymers to create cured films, are commonly employed as substitutes for usually volatile solvents. This substitution reduces the reliance on organic solvents, contributing to environmentally friendly practices

- UV-curable coatings enable room temperature curing, eliminating the need for high-temperature curing processes and contributing to energy conservation.
- UV-curable coatings are suitable for application on heat-sensitive substrates, making them ideal for use in plastic coatings and paper coatings etc.
- Compared to thermal curing, UV curing equipment is more compact, leading to higher efficiency and lower energy consumption, making UV curing a more economical.
- Mechanical and chemical stability of the prepared coatings is elevated due to the high cross-link density.
- Coatings prepared with UV rays undergo hardening usually through a radical mechanism, leading to rapid polymer radical reactions. This quick reaction time allows for fast and high-capacity production of coatings.
- After the UV-coating has hardened, no additional processing is required, costs are low**.**
- As the curing process takes place rapidly and uniformly, there is no alteration in the thickness of the coating.
- Coatings that harden with UV rays do not catch fire because they do not contain solvents [21, 51, 66].

Disadvantage:

- The high presence of some pigments that intensely absorb or reflect UV rays can make it difficult to prepare materials with UV rays. In the preparation of such films, although the surfaces of the films are dried, the inner parts do not dry sufficiently because UV rays cannot penetrate sufficiently into the inner parts.
- When there is difficulty in viscosity regulation, the excess amount of reactive diluent added changes the properties of the film.
- In cases where oxygen inhibits polymerization, coatings with lower mechanical properties can be obtained [21, 51, 66]**.**

1.5. Click Chemistry

The same polymerization method may not be suitable for all monomer combinations or functional groups. To address this, post-polymerization modification methods are employed, creating specific block copolymers or functional polymers by connecting polymer building blocks or adding functionality to a polymer precursor. Over the last two decades, click chemistry has significantly contributed to the development of these post-polymerization modification methods [67]. The term “click chemistry” was introduced by Sharpless et al in 2001 to characterize a set of exceptional reactions that exhibit numerous notable advantages, such as regioselectivity, exceptional yield, high efficiency, and tolerance to functional groups [68]. The most commonly used types of click reactions are copper-catalyzed 1,3 dipolar cycloaddition of azides and alkynes, thiol-ene reaction, Diels-Alder addition, epoxy ring opening reaction, aza-Michael addition and amino-yne addition [69]. Click reactions applied to vegetable oil triglycerides and their derivatives are shown below Figure 1.11.

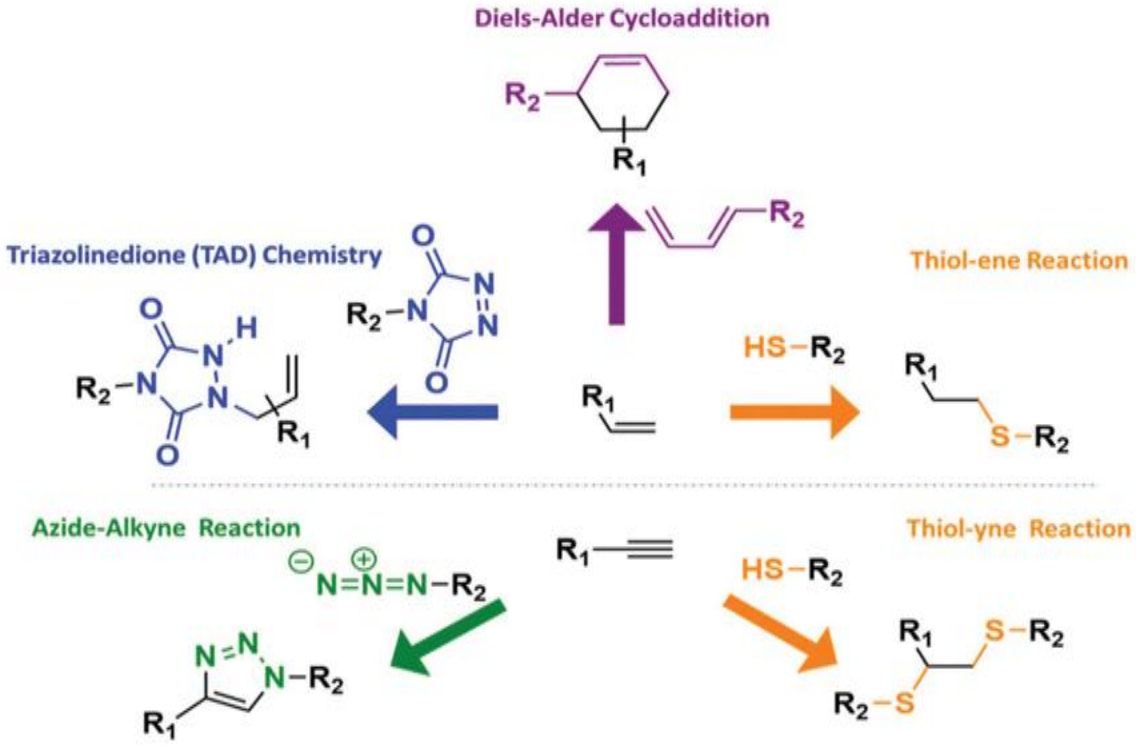


Figure 1.11. Schematic representation of click chemistry reactions [70].

Cu(I)-catalyzed azide–alkyne cycloaddition (CuAAC) click reactions are highly favored in polymer science due to their significant advantages, including high selectivity, quick and complete transformations, and orthogonality. These reactions are widely used for creating diverse polymer structures and functionalizing polymeric materials. The reactions are defined can occur either under transition metal-catalyzed conditions, specifically copper(I)-catalyzed alkyne–azide cycloaddition (CuAAC), or can be initiated by the inherent ring strain of cyclic alkynes [71]. The Diels-Alder cycloaddition involves a chemical reaction where a conjugated diene interacts with a substituted alkene, commonly known as a dienophile, resulting in the formation of an adduct. It is widely employed in the field of organic chemistry to generate six-membered unsaturated rings with a reasonable degree of control over regio and stereochemical properties [70]. Catalyst-free reaction conditions, the high efficiency, and thermo-reversibility are notable advantages of these reactions. Therefore, polymer science has widely utilized Diels–Alder reactions for the fabrication and functionalization of diverse macromolecular platforms [71].

1.5.1. Thiol-ene click chemistry

Among various UV-induced polymerization mechanisms, there has been a resurgence of interest in thiol-ene UV-curable formulations because of the inherent characteristics of these reactions. The formulations involve a combination of multifunctional ene monomers and multifunctional thiols, initiating step-growth polymerization upon UV irradiation, resulting in crosslinked networks [72]. Thiols, acknowledged as transfer agents, can undergo a reaction with alkenes through photochemical or thermal initiation at room temperature, in the presence of oxygen, without giving rise to undesirable side reactions like sulfenyl radical coupling. Significantly, these reactions can be regarded as environmentally friendly processes as they occur in the absence of a solvent, under mild reaction conditions, and without the involvement of any potentially toxic metals [73]. In addition, the characteristics of thiol–ene networks can be readily controlled by selecting particular monomers. In general, the thiol–ene reaction can be viewed as a more cost-effective and environmentally friendly approach to produce biobased flexible polymers. The thiol-ene reaction exploits the labile sulfur–hydrogen bond, and two reactions between thiols and double bonds have become widespread:

i. The thiyl radicals generated from thiols through initiation by light, heat, or radical initiators, undergo free-radical addition to electron-rich or electron-poor double bonds.
ii. The catalysed thiol-Michael addition of a thiol to an electron-deficient carbon-carbon double bond [74].

Additionally, a notable characteristic of this reaction is that nearly any alkene functional group can engage in it. The reaction proceeds by a free radical chain mechanism that may be started by UV radiation or radical initiators, resulting in mainly anti-Markovnikov products. Nevertheless, it is crucial to emphasize that the addition of thiyl radicals to olefins is a reversible process, potentially resulting in cis/trans isomerization of the initial substance [75]. The thiol-Michael addition is regarded as a highly efficient "click" type reaction, extensively employed in the synthesis and functionalization of polymer materials. The thiol-ene radical polymerization mechanism begins with the initiation of a thiol radical through the abstraction of hydrogen from a thiol. Generally, thiol-ene reactions occur under radical conditions using thermal or photodegradable initiators. The reaction initiates through the radicals generated by these initiators. The formation of the thiyl radical (RS^{o}) occurs when hydrogen is abstracted from the thiol structure by the radicals generated through the decomposition of initiators, either by heat or photochemical means. In the progressive step, the thiyl radical is clamped to the C=C double bond, forming a carbon-centered intermediate in radical form. In the end, the carbon-centered radical breaks the hydrogen of another thiol, resulting in the formation of the final product **[76].** Figure 1.12 below shows the general radical thiol-ene reaction mechanism.

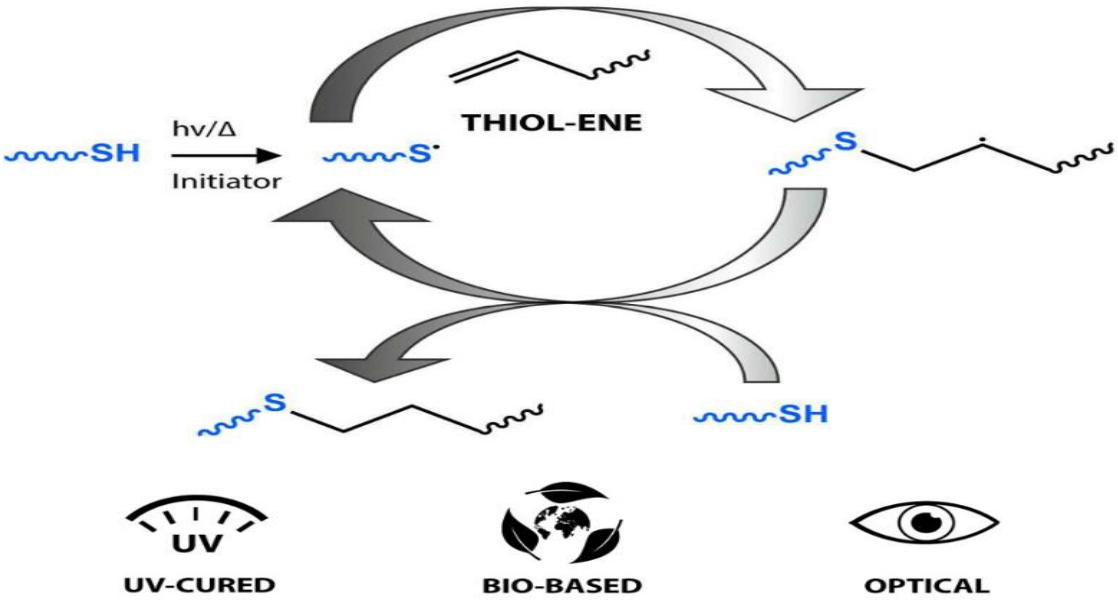


Figure 1.12. General radical thiol-ene reaction mechanism [76].

1.5.1.1. Advantages and disadvantages of thiol-ene click chemistry

It has garnered growing attention in recent years because of its recognition as a "click chemistry" method, characterized by easy product isolation regiospecificity, high yields, and mild reaction conditions using readily available starting materials and reagents. The reaction's flexibility is aided by the fact that it does not require a catalyst, may be started both thermally and photochemically, and tolerates a wide range of functional groups. Thiol-ene click reactions can be conducted without the use of solvents and catalysts, and the resulting products can be readily purified in high yields [77]. In addition to these features, UV-curable formulations utilizing thiol-ene functionality present numerous benefits, including the absence of oxygen inhibition, highly uniform networks, delayed gel points, enhanced polymerization control, diminished polymerization shrinkage, and reduced stress. The thiol-ene click reaction proceeds in the presence of air nearly as rapidly as in an inert atmosphere. As thiol groups react with peroxide radicals and generate highly reactive thiyl radicals through the absorption of hydrogen by peroxide radicals, the issue of oxygen inhibition is essentially resolved [78].

However, besides its advantages, it also has some disadvantages. Similar to other cross-linked polymers, the structure of thiol–ene networks poses the challenging issue of being hard to recycle, leading to resource inefficiency and environmental pollution. Concretely,

the cross-linked structures cannot undergo reprocessing or decomposition under mild conditions as they are unable to melt and become insoluble after curing [74]. In addition, the bad odor of the thiol components used, low Tg, and low durability of the prepared materials can be shown as disadvantages of the system [79].

1.5.1.2. Thiol-ene coatings containing vegetable oils

In recent times, there has been a growing interest in substituting petroleum-based monomers with bioresources, driven by mounting environmental concerns and the anticipation of dwindling petroleum resources. High-performance coatings utilizing thiol-ene chemistry have already been successfully developed using biobased monomers, including terpenes, unsaturated vegetable oils, and derivatives of lignin [72]. Thiol-ene click chemistry has been widely utilized in various applications, including the modification of vegetable oils. The versatility and mild conditions of thiol-ene click chemistry make it a promising tool for introducing functional groups into vegetable oils, thereby enabling the development of biobased materials [80]. UV curable materials derived from plant oils exhibit inherent “softness” due to the long fatty chains, leading to a lower glass transition temperature (Tg). This characteristic restricts the applicability of plant oil-based materials in durable applications. Studies are being carried out aiming to further develop these bio-based UV-curable materials and increase their Tg and performance [65]. Black et al. Vegetable oil acrylates produced from castor oil were combined with a trifunctional thiol and cross-linked using UV light. Each biobased monomer has been shown to display outstanding performance in thin film applications within UV-curable thiol-ene formulations and has been suggested for improving physical characteristics. It has been proposed that coatings curable with thiol-ene, incorporating vegetable oil macromonomers as prepolymers, could be beneficial for applications demanding sustained flexibility, such as in paper coatings, coil coatings and optical fiber coatings [78].

1.5.1.3. Thiol-anhydride dynamic reversible networks

It has been demonstrated that the ring-opening reaction between thiols and anhydrides results in the formation of thioesters/acids, which exhibit high reversibility. Consequently, networks employing adaptive dynamic covalent chemistry have been

developed. These covalent adaptive networks offer self-healing properties to covalent bonds while retaining typical thermoset properties and solvent insolubility. By subjecting them to external stimuli such as temperature, light, or pH changes, these thermosets can be reshaped or reused. Previous research has indicated that thiols and thioesters within the polymer network structure, predominantly derived from monomers resulting from the ring opening of succinic anhydride with 3-mercaptopropionic acid, undergo dynamic changes at various temperatures [88].

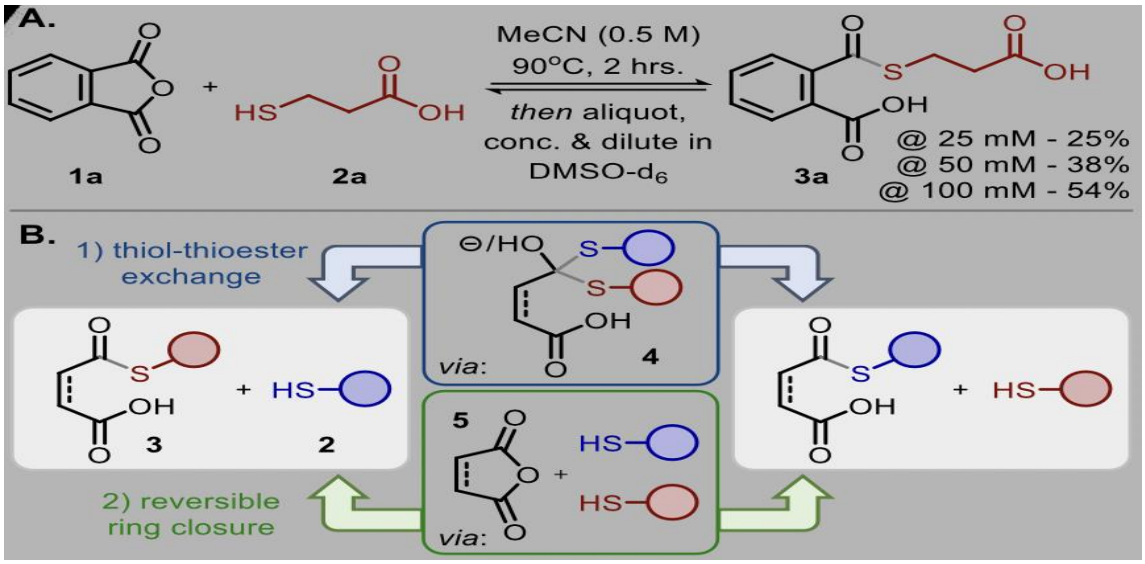
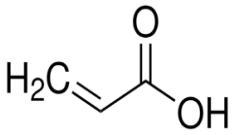


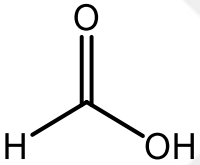
Figure 1.13. A. The unexpected concentration-dependent inversion of the thiol-anhydride reaction in a polar environment, as corroborated by 1H-NMR evidence; **B.** suggested potential mechanisms for the reversible addition of thiols to anhydrides, either through thiol-thioester exchange (1) or reversible anhydride ring closure (2) [88].

2. MATERIAL AND METHOD

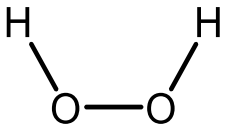
2.1. Chemicals and Materials Used



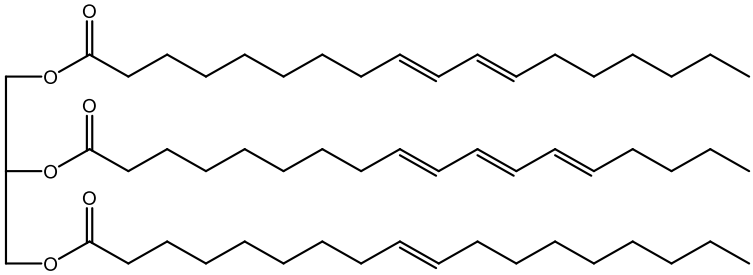
Name : Acrylic acid
Supplier : Merck KGaA
Closed Formula : C3H4O2
Boiling Point : 141 °C
Density : 1.05 g/cm3
Molecular Weight : 72.06 g/mol



Name : Formic acid
Supplier : Merck KGaA
Closed Formula : CH_2O_2
Boiling Point : 101 °C
Density : 1.22 g/cm3 (20 °C)
Molecular Weight : 46.02 g/mol



Name : Hydrogen peroxide
Supplier : Merck KGaA
Closed Formula : H_2O_2
Boiling Point : 107 °C
Density : 1.11 g/cm3
Molecular Weight : 34.01 g/mol



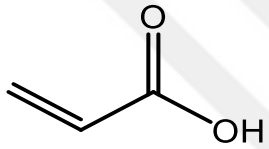
Name : Linseed oil

Supplier : Yeni Turan Bezir Yağ San. Ve Tic. A.Ş

Closed Formula : $C_{57}H_{98}O_6$

Density : 0.9304 kg/m^3

Molecular Weight : 879.40 g/mol



Name : Acrylic acid

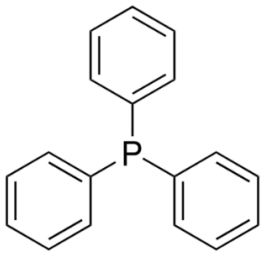
Supplier : Sigma Aldrich

Closed Formula : $C_3H_4O_2$

Boiling Point : 141 °C

Density : 1.05 g/cm^3

Molecular Weight : 72.06 g/mol



Name : Triphenyl Phosphine

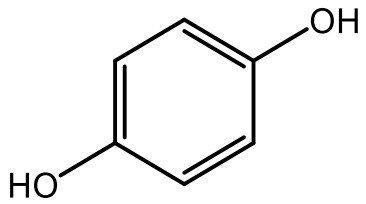
Supplier : Henkel

Closed Formula : $C_{18}H_{15}P$

Boiling Point : 377°C

Density : 1.1 g/cm3

Molecular Weight : 262.29 g/mol



Name **:** Hydroquinone

Supplier **:** Merck KGaA

Closed Formula **:** $C_6H_6O_2$

Boiling Point **:** 287 °C

Density **:** 1.332 g/cm3

Molecular Weight **:** 110.11 g/mol



Name **:** Maleic anhydride

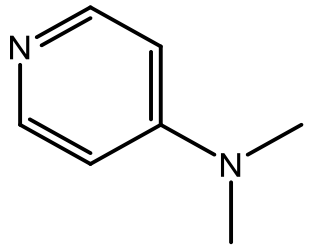
Supplier **:** Sigma- Aldrich

Closed Formula **:** $C_4H_2O_3$

Boiling Point **:** 200 °C

Density **:** 1.48 g/cm3

Molecular Weight **:** 98.06 g/mol



Name **:** 4-Dimethylaminopyridine

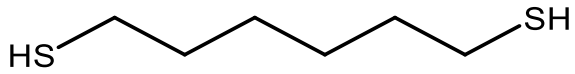
Supplier **:** Sigma Aldrich

Closed Formula **:** $C_7H_{10}N_2$

Boiling Point **:** 138-140 °C

Density **:** 0.906 g/mL at 25 °C

Molecular Weight **:** 122.17 g/mol



Name : 1,6-Hexanedithiol

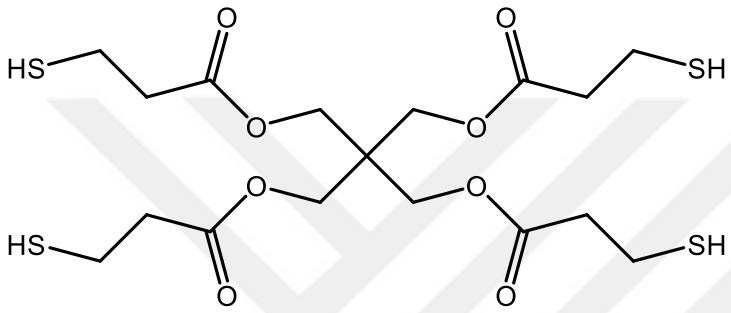
Supplier : Sigma Aldrich

Closed Formula : $C_6H_{14}S_2$

Boiling Point : 118-119 °C

Density : 0.983 g/mL at 25 °C

Molecular Weight : 150.30 g/mol



Name : Pentaerythritol tetrakis(3-mercaptopropionate)

Supplier : Aldrich

Closed Formula : $C_{17}H_{28}O_8S_4$

Boiling Point : 275 °C

Density : 1.28 g/ml

Molecular Weight : 488.64 g/mol

2.2. Devices and Equipment Used

2.2.1. Fourier transform infrared (FT-IR) spectroscopy

Structure characterization was examined with the ATR method using the SHIMADZU - IRSpirit™ brand device.

2.2.2. Nuclear magnetic resonance spectroscopy (1H-NMR)

In order to examine the structural analysis of the synthesized AELO and Thiol in detail, the Varian Mercury-VX 400 MHz BB brand +H-NMR device located at Boğaziçi University was used.

2.2.3. Water contact angle

To investigate the hydrophobic qualities of the coatings formed on the glass layer, the contact angles of the films with water drops were measured using the KRUSS DSA 10 equipment.

2.2.4. Tensile rupture test

It is aimed to measure the mechanical performance of the films obtained with the Zwick Roell BDO-FB0.5TH brand device. The test was applied with 100% deformation, preload of 5 N and test speed of 10 mm/min.

2.2.5. Differential scanning calorimeter (DSC)

PerkinElmer brand Diamond model DSC device was used to determine the glass transition temperature (Tg) values of the prepared free films. Samples of 5-10 mg from each of the prepared free films were weighed and placed in aluminum pans. DSC studies of the samples were cycled 2 times in hermetically sealed aluminum pans, ranging from 20 °C to 100°C. The glass transition temperature was determined as the midpoint of the gradual transition from the second heating.

2.2.6. Thermogravimetric and differential thermal analyzer (TG/DTA)

Thematic analysis of the prepared compositions was performed on the PerkinElmer Diamond TG/DTA brand device at Yıldız Technical University.

2.2.7. Pencil hardness test

By drawing the coating surface with a pencil of different hardness, the level of surface hardness was measured depending on the streching on the surface. Pencils have different hardness levels between 1H-7H.

2.2.8. Cross-cut test

To measure the adhesion performance, the adhesion level of the surface was measured with a standard tape after scratching (#) on the coating vertically and horizontally, using an cross cutting device specific to the ASTM-D3359-2017 standard.

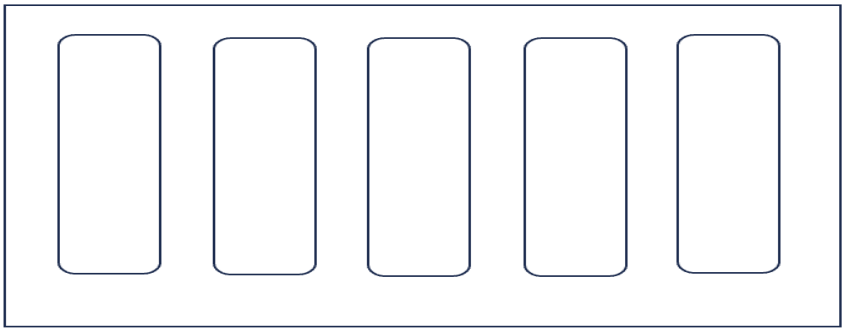
2.2.9. Pendulum test

A hardness test was performed on the surfaces coated with the BYK Gardner brand in the Konig/sec unit of measurement.

2.3. Equipment

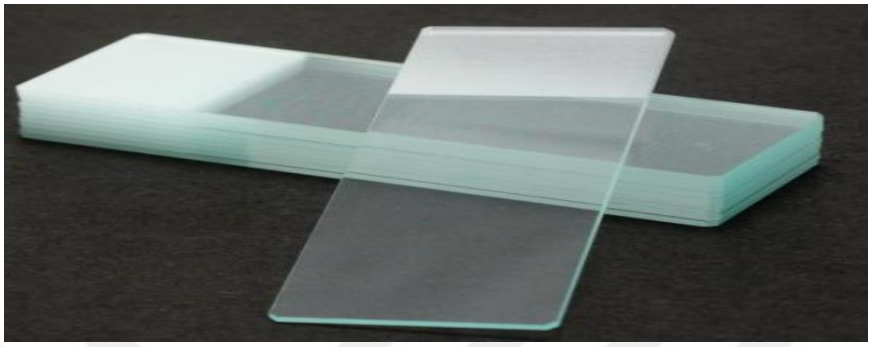
2.3.1. PTFE mold

It is designed to obtain a free film by pouring the prepared formulations into the compartments on the Teflon mold.



2.3.2. Glass plate

Glass plates with dimensions of 26 x 76 x 1 mm are the preferred substrate micro glass materials for creating thin films. This process can be carried out using the glass baguette method.



3. EXPERIMENTAL METHOD

3.1. Synthesis of Epoxidized Linseed Oil (ELO)

The epoxidation of flaxseed was carried out in a 3-necked glass bottle using a mechanical stirrer, thermometer, and dropping funnel. First, after the system was set at 50 °C, 50 ml of flaxseed oil and 15 ml of Formic acid were added to the glass material and mixed at 500 rpm. Then, 80 ml of Hydrogen peroxide (H2O2) was slowly added to the system through the drop funnel for 1 hour. After the addition process was completed, mixing was continued at 50 °C and 500 rpm for 18 hours. The synthesized epoxidized linseed (ELO) was first dissolved in 30ml of diethyl ether. Then, in order to remove unreacted Formic acid and H_2O_2 substances remaining in the ELO, washing was carried out with saturated sodium bicarbonate solution until the pH was 7, and then washing was performed again with the prepared saturated NaCl solution. Then about 2 spatulas of Sodium sulphate were used to remove excess water and the product was separated with decantation. The ethyl ether we used was removed at a rotary evaporator at 50 °C at 230 rpm.

Table 3.1. Raw materials used in the synthesis of epoxidized linseed oil

Raw Materials Used	Amount Used
Flaxseed Oil	50 ml
Formic Acid (%98)	15 ml
H2O2 (%35)	80 ml

3.2. Acrylation of Epoxidized Linseed Oil

The acrylation process is based on the ring-opening procedure of the oxirane group in epoxidized linseed oil using acrylic acid. Here, the amount of acrylic acid equal to the percentage of oxirane formed will be used, and since it is aimed to open the entire percentage of oxirane formed with acrylic acid, a 1:1 ratio was calculated as stoichiometric. A 2-neck glassware was taken and our main component ELO (20 grams) was mixed with Triphenyl phosphine (0.40 grams) as catalyst and Hydroquinone (0.04 grams) as free radical inhibitor for 1 hour at room temperature. Acrylic acid (5.170 grams), used as ring-opening agent, was added dropwise for about 40 minutes at room temperature. After all additions were made, the apparatus was brought to 80 °C and mixed

for another 5 hours. During this period, the process was carried out in a foil-wrapped condition so that the product does not get light. The synthesis procedure is given in Table 3.2.

Table 3.2. Raw materials used in the synthesis of AELO

Raw Materials Used	Amount Used
ELO	20 grams
Acrylic Acid	5,170 grams
TPP	0,40 grams
Hydroquinone	0,04 grams

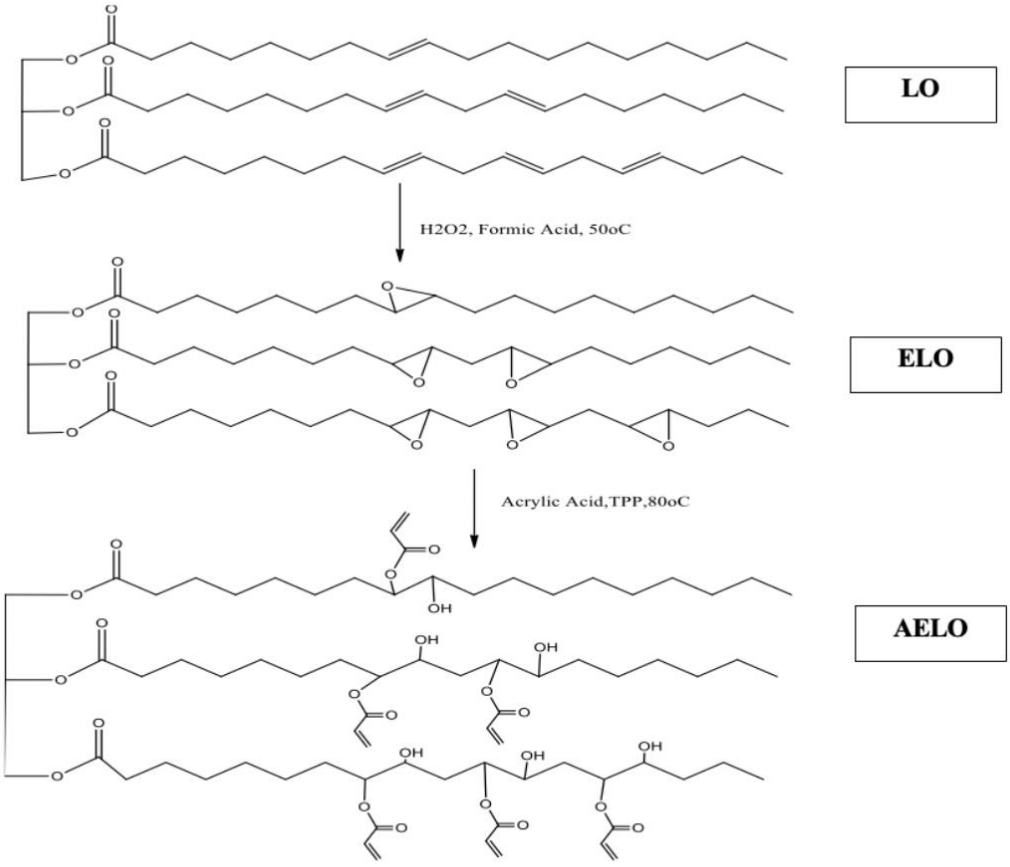


Figure 3.1. Acrylation of epoxidized linseed oil

3.3. Synthesis of Thiol Compound

Maleic anhydride and DMAP (%5) were loaded into a clean and dry two-necked flask, and acetone, the substance in which they were soluble was added. The 1,6-hexanedithiol

(2SH) product was added dropwise for about 20 minutes at room temperature and stirred for 1 hour. Then the temperature was brought to 50 °C and mixing was carried out for another 2 hours. After thiol synthesis was done, it was kept under vacuum to remove acetone. The synthesis procedure is given in Figure 3.2.

Table 3.3. Raw materials used in the synthesis of thiol compounds

Raw Materials Used	**Amount Used**
Maleic Anhydride	5 grams
1,6 hexanedithiol	7,515 grams
DMAP (%5)	0,65 gram

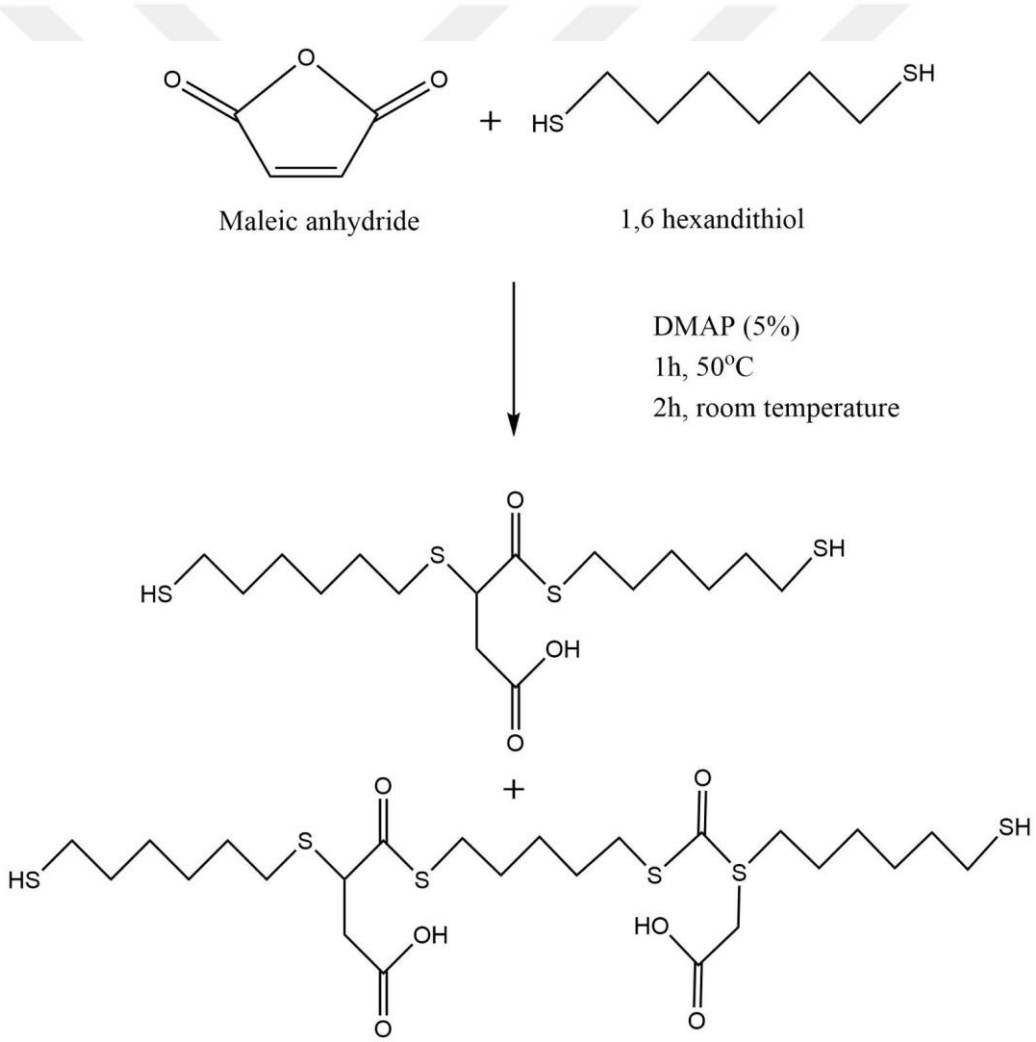


Figure 3.2. Synthesis scheme of thiol compounds

3.4. Preparation of UV Curable Films with Thiol-Ene Click Chemistry

The formulation of UV curing films prepared by using the synthesized AELO resin and thiol compound together with different ratios of commercial Pentaerythritol Tetrakis (4SH) material is given in Table 3.4 below.

Table 3.4. Formulations of UV cured films

Test Number	AELO	Thiol Compound	Pentaerythritol Tetrakis	PI (%)
F1	5 gr	1,18 gr	-	3
F2	5 gr	1,18 gr	0,21 gr	3
F3	5 gr	1,18 gr	0,42 gr	3

After all the products were taken in determined amounts, they were mixed homogeneously by adding photoinitiator. After, they was poured into Teflon molds and UV curing process was carried out. The UV cured films were then kept in an oven at 120 °C for 1 hour and 24 hours with postcure application, and the curing process was continued and mechanical and thermal comparisons were made. The thiol compound synthesized in our thesis from maleic anhydride and 1,6-hexanedithiol was specifically designed to introduce dynamic covalent bonds into the vegetable oil-based thiol-ene coating. As established in prior studies, the presence of free thiols in the reaction medium can facilitate thiol-thioester exchange, leading to increased cross-linking and ultimately resulting in the formation of networks that are more effective at reducing stress.

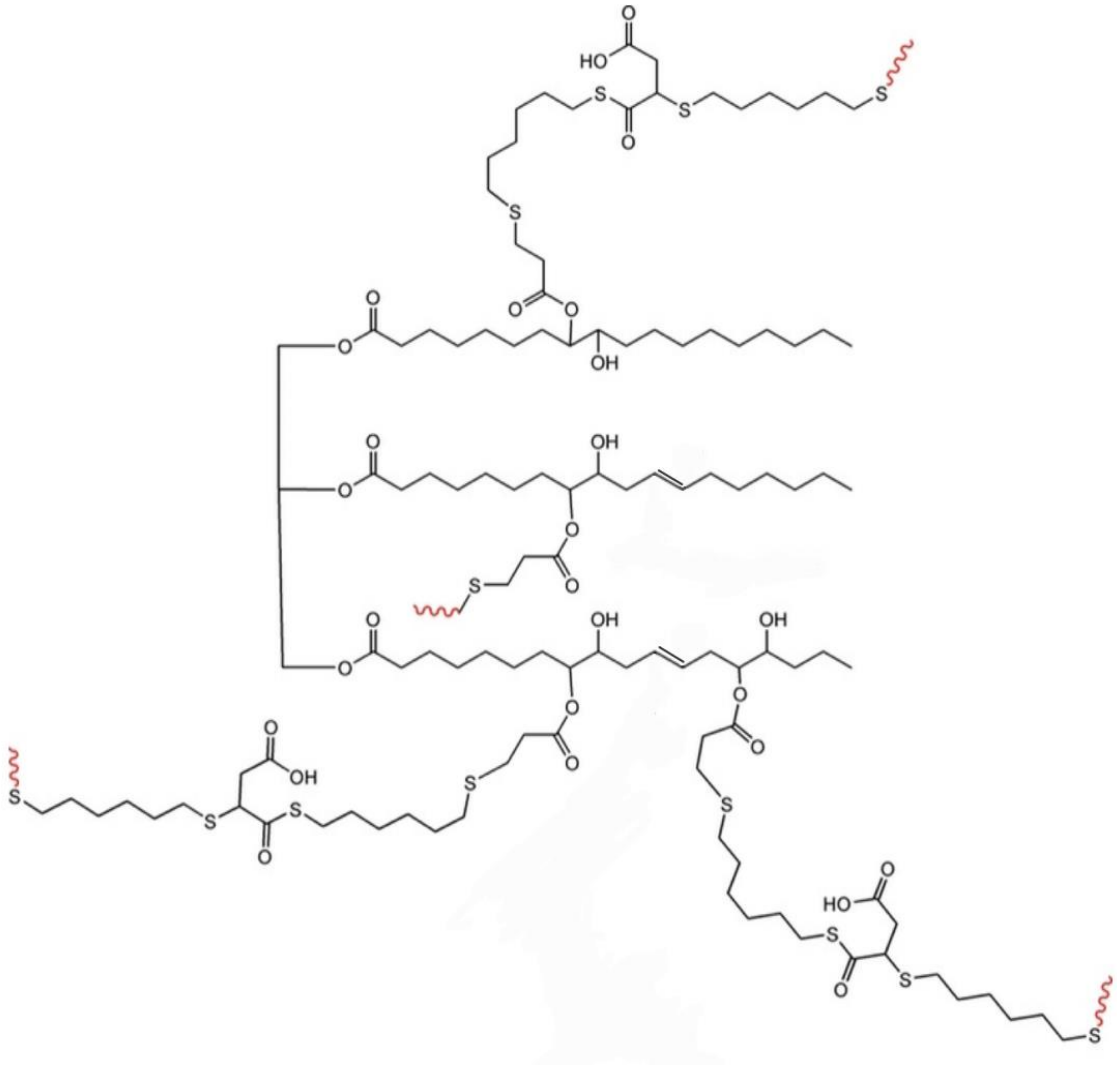


Figure 3.3. Chemical structure of UV curable F1 formulation film with thiol-ene click chemistry

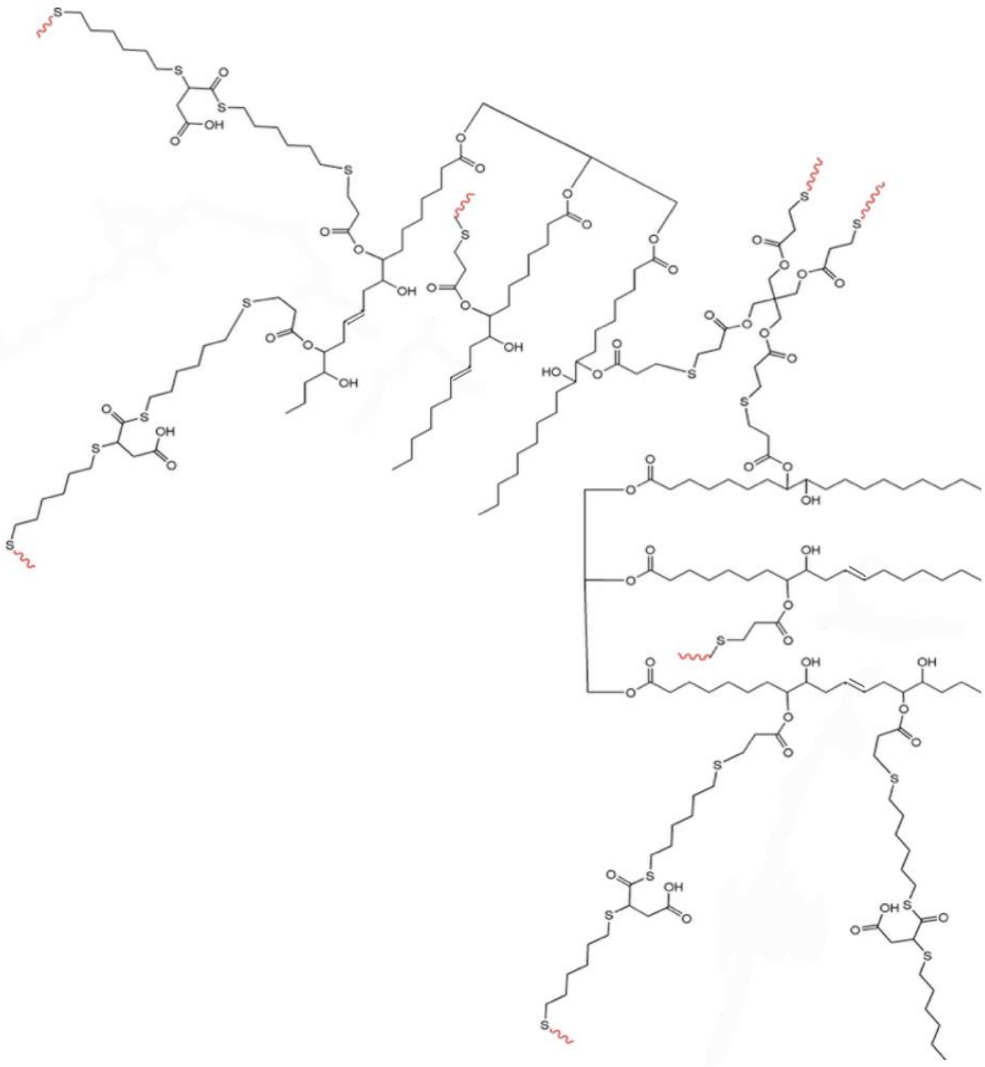


Figure 3.4. Chemical structure of UV curable F2 and F3 formulation film with thiol-ene click chemistry

4. RESULTS AND DISCUSSION

4.1. FTIR Analysis of Epoxidized Linseed Oil

Carbon-Carbon double bonds in flaxseed are the main reaction zone, and new functional groups can be formed by making various modifications in these regions. Bio-based resin can be synthesized by using double bonds on the fatty acid, since flaxseed epoxidation is the reactive main substance to form new functional groups. The use of formic acid in the epoxidation process ensures that the carbon-carbon double bond in the fatty acid is broken and the oxirane ring is formed.

When we compare the FTIR analysis result of linseed oil and Epoxidized linseed oil in the chart numbered Figure 4.1 below, we observe the changes in the structure of unsaturated fatty acids in the triglyceride molecule. Examining the LO spectrum, the peak at 1742 cm^{-1} indicates C=O stretching and the signal at 1159 cm^{-1} indicates C-O stretching. The peak at 2852.16 cm^{-1} confirms the presence of the CH2 group. Another functional group belonging to flaxseed, C=C, peaks at 1654 cm^{-1}. Examining the FTIR spectrum of ELO, the Carbon-Carbon double bond at 1654 cm^{-1} from Flaxseed is almost not visible in ELO, indicating that the double bonds are broken by epoxidation. Signals indicating that the double bonds are broken with epoxidation and C-O-C stretching of the oxirane ring is formed are observed with the peak located at 822 cm^{-1} [81, 82].

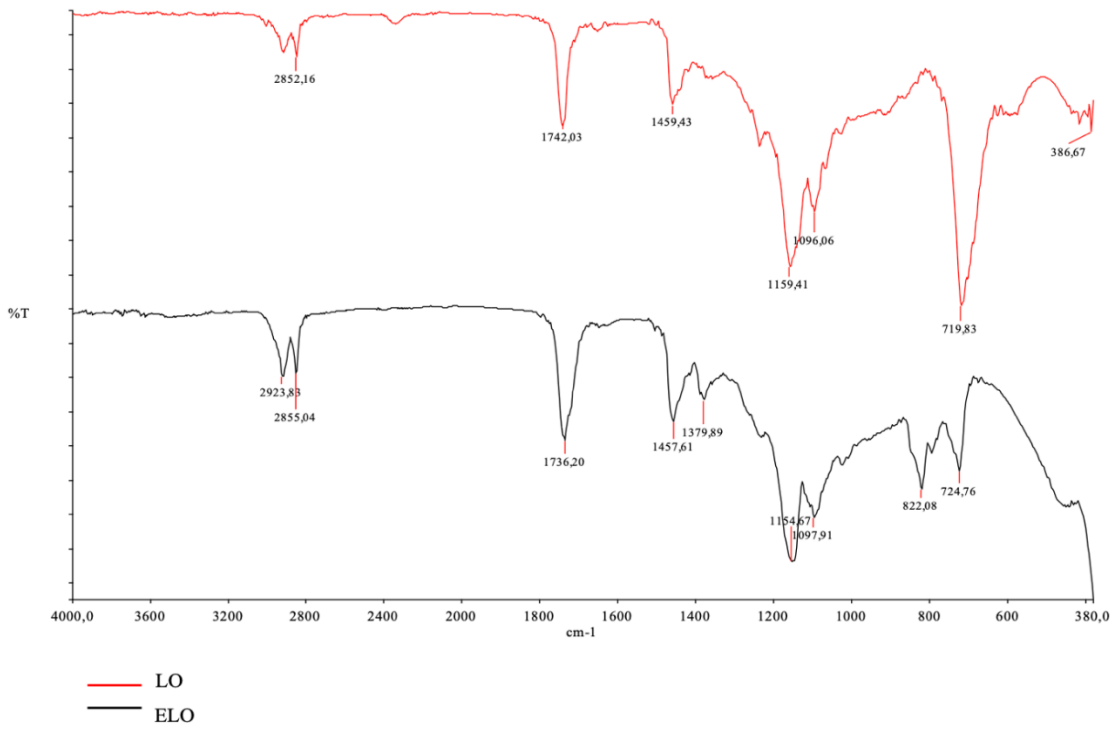


Figure 4.1. FTIR analysis of epoxidized LO and linseed oil

Oxirane Oxygen Content:

The oxirane oxygen content functions as a gauge for the extent of epoxidation, reflecting the number of epoxy units present within the resin. This content can be determined analytically theoretically and instrumentally. The highest achievable theoretical oxirane oxygen content can be approximated using below equation.

$$OO_t = \left\{ \frac{\left[\frac{IV_0}{2A_i}\right]}{100 + \left[\frac{IV_0}{2A_i}\right] A_0} \right\} \times A_0 \times 100$$

Where;

Ai: It has a value of 129.9 and is the atomic weight of iodine.

A0: It has a value of 16.0 and is the atomic weight of oxygen.

IVo: It represents the oil sample's initial iodine value.

The analytical determination of the degree of epoxidation involves titration with a hydrogen bromide solution. Hydrogen bromide initiates epoxide ring opening via

bromination, leading to the formation of a hydroxyl group. After all epoxide groups have undergone reaction, the color of the used indicator changes owing to the presence of unbound hydrogen bromide (produced by an excess of perchloric acid) This approach quantifies the epoxide group content and consequently evaluates the conversion to the desired product. [31]. In this experiment, the oxirane value of epoxidized flaxseed was found to be 7.9%.

4.2. FTIR and ^{1}HNMR Analysis of Acrylization of ELO

The epoxide rings formed by the epoxidation of flaxseed are opened with the use of acrylic acid, which is a ring-opening agent and as a result, AELO synthesis occurs by attaching the acrylate and hydroxyl groups to the triglyceride molecule. When the FTIR spectrum of the above AELO is examined in the chart number Figure 4.2 below, the peak at 1719 cm^{-1} shows that there is a C=O stretch belonging to the carbonyl group. The stretching of the vinyl group (-CH =CH_2) in acrylate occurs at peaks located at 812 cm^{-1}, 984 cm^{-1} and 1408 cm^{-1}. The peak at 1633 cm^{-1} comes from the functional group of the C=C stretch. As a result, it was observed that the peaks belonging to the epoxy group disappeared after the acrylation process [81, 82].

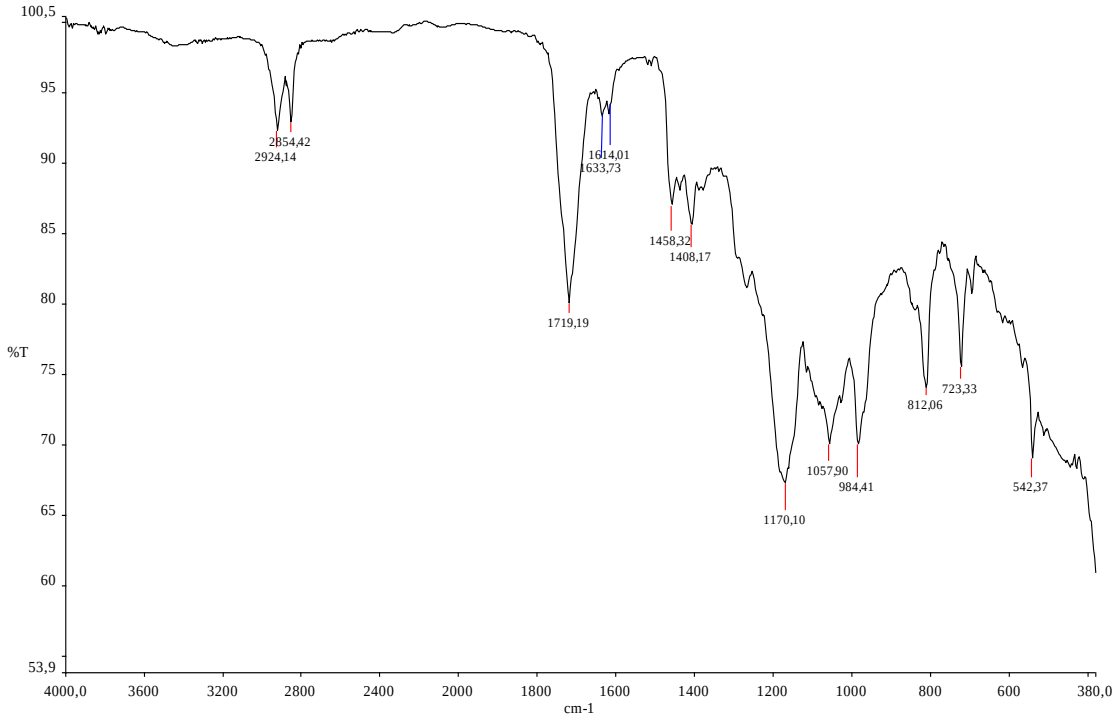


Figure 4.2. FTIR spectra of acrylization of ELO

The epoxy groups exhibit chemical shifts at 2.8-3.3 ppm in nuclear magnetic resonance (NMR) spectra. Upon modification of the resin samples, these epoxy signals become undetectable, while new signals emerge along the polymer chain after acrilation thereby providing evidence of successful acrylation-induced modifications.Acrylate groups evidenced by peaks at d = 5.6 to 6.4 ppm. These peaks signify the three protons linked to the carbon-carbon double bond of the acrylate esters [43, 81].

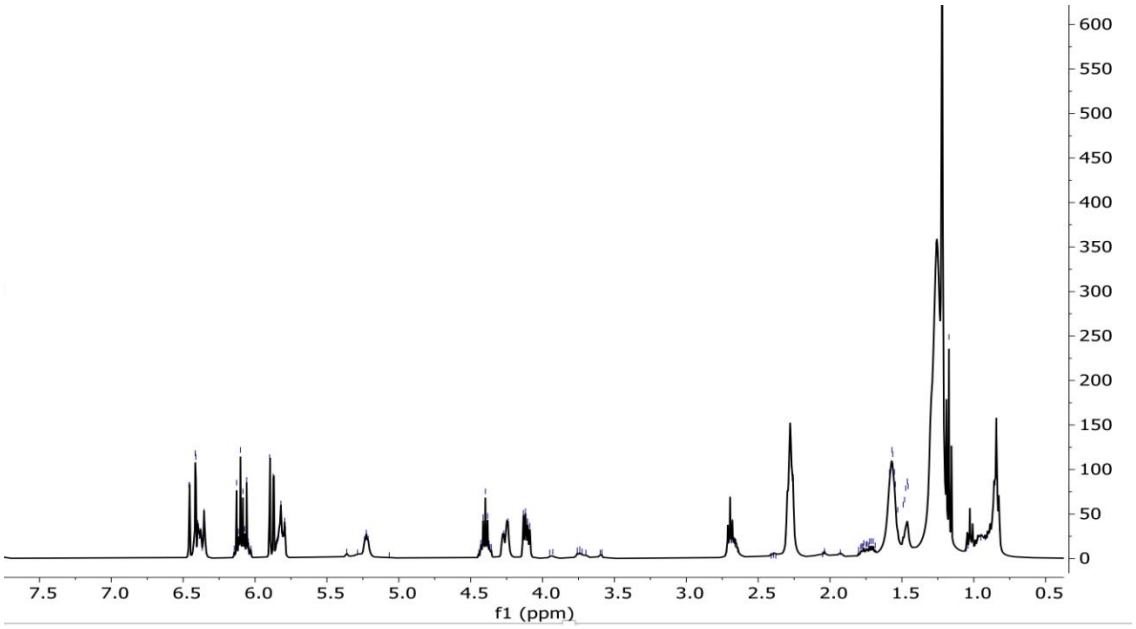


Figure 4.3. ^{1}HNMR spectra of acrylated epoxidized linseed oil

4.3. FTIR and ^{1}HNMR Analysis of Thiol Compound

FTIR analysis of the thiol compound synthesized using maleic anhydride is given in the Figure 4.4 below. When examining the spectra of maleic anhydride, it was observed that carbonyl on the five-membered ring of the maleic anhydride carbonyl peaked at 1854 cm^{-1}. The anhydride ring must be opened with the formation of thiol synthesis. When the spectrum of the synthesized thiol compound is investigated, the disappearance of the peak at 1854 cm^{-1} of the maleic anhydride during the thiol synthesis shows that the anhdyride ring is opened and thiol synthesis has taken place [83]. The peak manifesting at 2568 cm^{-1} (S-H) is attributed to thiol groups, corroborating the synthesis of thiols [84]. 1671 cm^{-1} multiple carbonyl peaks indicate carboxylic acid and carbonyl adjacent to sulfur.

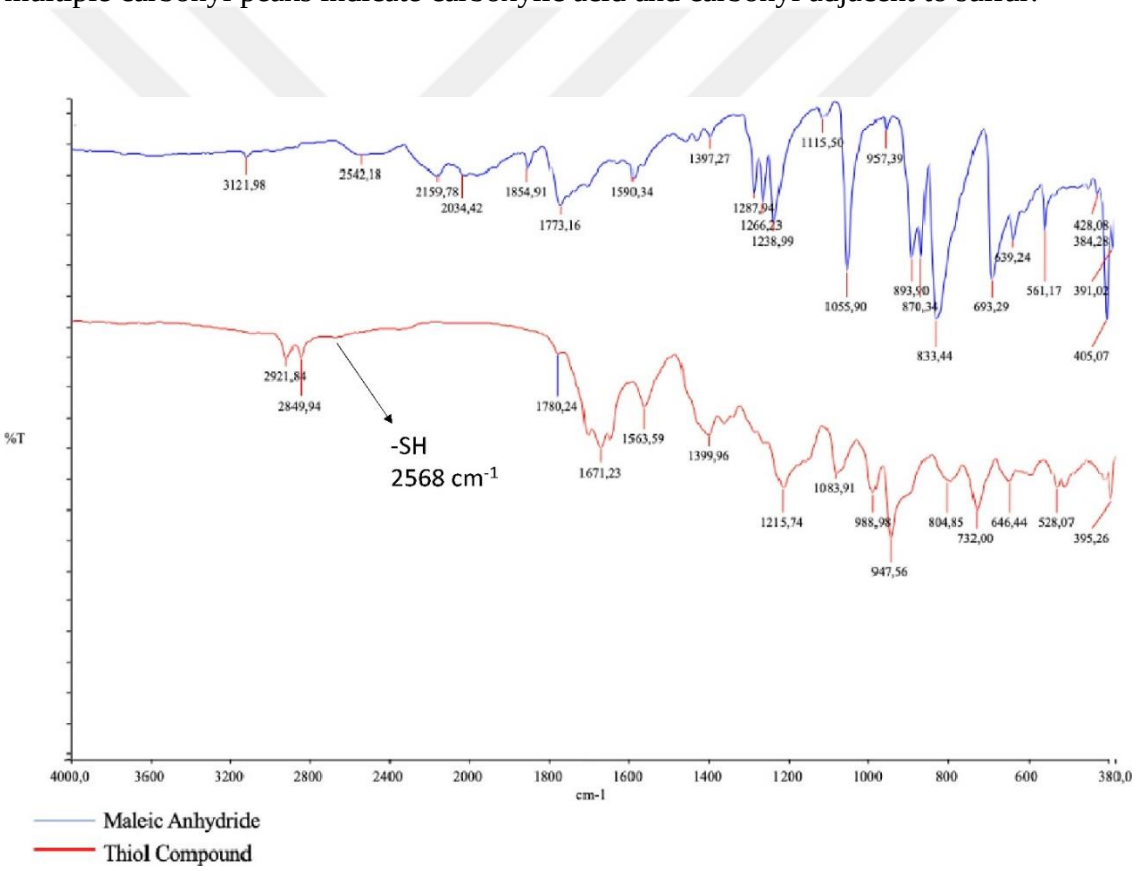


Figure 4.4. FTIR spectra of thiol compound

Hydrogen atoms situated on carbon atoms neighboring the sulfur atom in thiols are typically observed in the chemical shift range of 2.5 ppm [89]. As seen in Figure 4.5 below, the peak at 2.5 ppm confirms this information. As seen in figure 4.5 below, the SH hydrogen of the thiol was seen at 1.33 ppm. This situation peak shows that the thiol molecule is synthesized successfully. In addition, when the other peaks are examined, protons bound to CH2 groups are seen at 1.6, 3.18, 3.30 and 3.90.

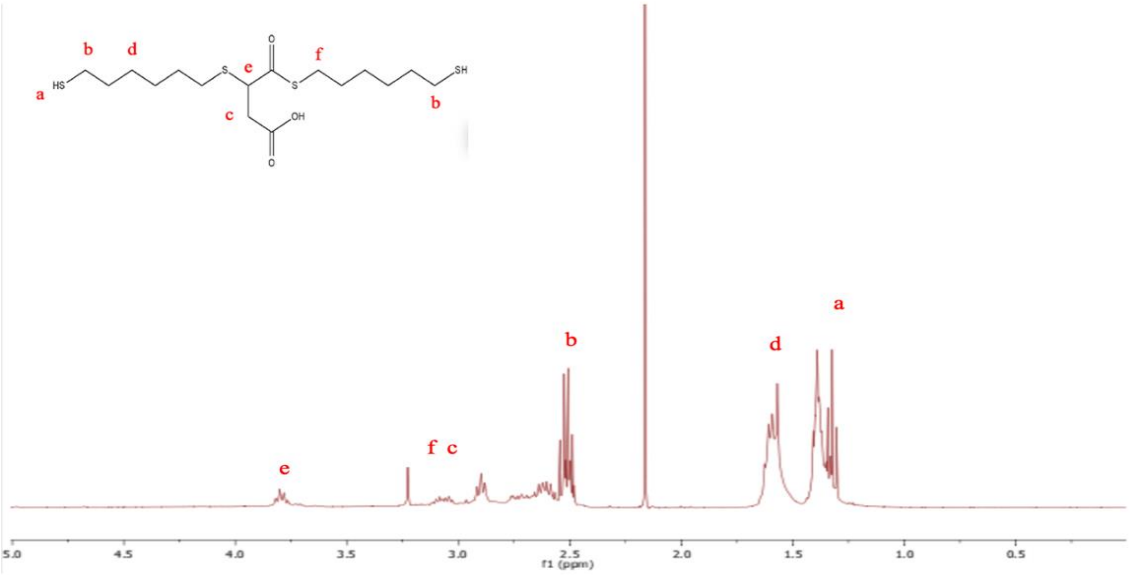


Figure 4.5. ^{1}HNMR spectra of thiol compound

4.4. FTIR Analysis of Prepared Films

UV curable films were prepared using thiol ene click chemistry and a comparison was made by applying postcure at different times. The films given in the FTIR spectrum above were compared in Figure 4.6. The thioester carbonyl bond, which is present in 1690 cm-1 in UV-cured films, decreased in these peaks as the amount of thermal heat received by the film at 120 degrees increased [85]. No difference was observed between the IRs of Pentaerythritol Tetrakis (4SH) films used in different ratios. For this reason, each film was interpreted by comparing it within itself.



Figure 4.6. FTIR Spectra of F1 Formulation Films

4.5. Performance Properties of Prepared Films

4.5.1. Differential scanning calorimetry device (DSC)

In general, the Tg of thiol-ene light-cured systems is low due to is added thiol compound. [86]. As observed in the results, the Tg values of the films containing the -SH group cross-linked with UV light were found to be 11.31, 7.1, and 1.9 °C. The aliphatic flexible chains originating from this structure reduced the Tg as pentaerythritol tetrakis (4SH) monomer was added to the film mixture in increasing amounts. Since increasing the -SH content would increase cross-linking, it was expected to increase Tg. However, it has been

observed that aliphatic chains dominate in reducing Tg by providing flexibility. The cross-link density increased and the Tg value increased in the samples subjected to thermal curing after UV curing. Previous research has demonstrated that the presence of free thiols in the reaction medium can promote thiol-thioester exchange, which in turn increases cross-linking and eventually leads to the development of higher stress-reduction-efficient networks.

Table 4.1. DSC analysis results of prepared films

SAMPLE	Tg (°C)	Cp(J/g°C)
F1-UV	11 ,31	0.097
F1-UV+1h	11 ,69	0.145
F1-UV+24h	17	
F2-UV	7.1	0.012
F2-UV+1h	17.79	0.022
F2-UV+24h	18.21	0.011
F3-UV	1.9	0.023
F3-UV+1h	8 ,95	0.139
F3-UV+24h	19.2	0.01

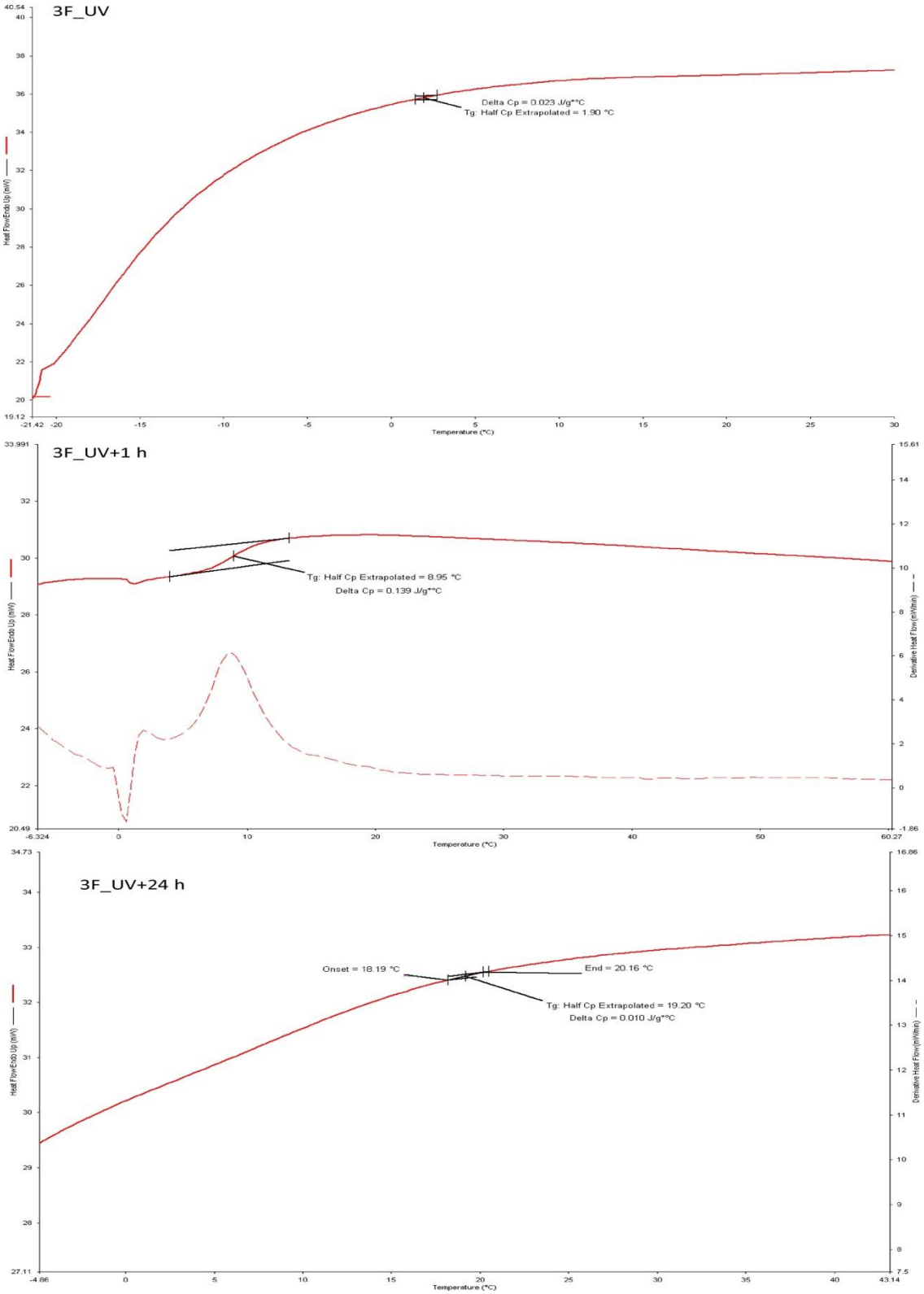


Figure 4.7. DSC analysis results of prepared F3 formulations

4.5.2. TG-DTA analysis of prepared films

To determine the thermal stability of the films, TGA analysis was conducted under air, with a heating rate of 20 °C per minute across a temperature range of 30–750 °C. The resulting thermogram profiles can be seen in Figure 20. Based on the TGA thermogram profiles, it was observed that the main degradation process of the films started at approximately 261° C. The approximately 1-2% mass loss observed in all samples below 200° C is due to the evaporation of moisture and water that may be commonly present in the samples. Moreover, the initial degradation temperature of the films increased up to 280 °C with the increase of -SH content. While the 90% maximum mass loss is 484 °C for the PETMP-free film (F1), this value is 487 ° C for the PETMP-containing F3 film. These findings indicate that the films are heat resistant and the main degradations occur above 300 °C. Therefore, these films can be considered safe and suitable for various coating applications.

Table 4.2. TGA analysis evaluation of prepared films

SAMPLE	T5 (°C)	T50 (°C)	RESIDUE (%) @ 700 (°C)
F1	261	391	0.89
F2	265	392	0.92
F3	280	392	0.84

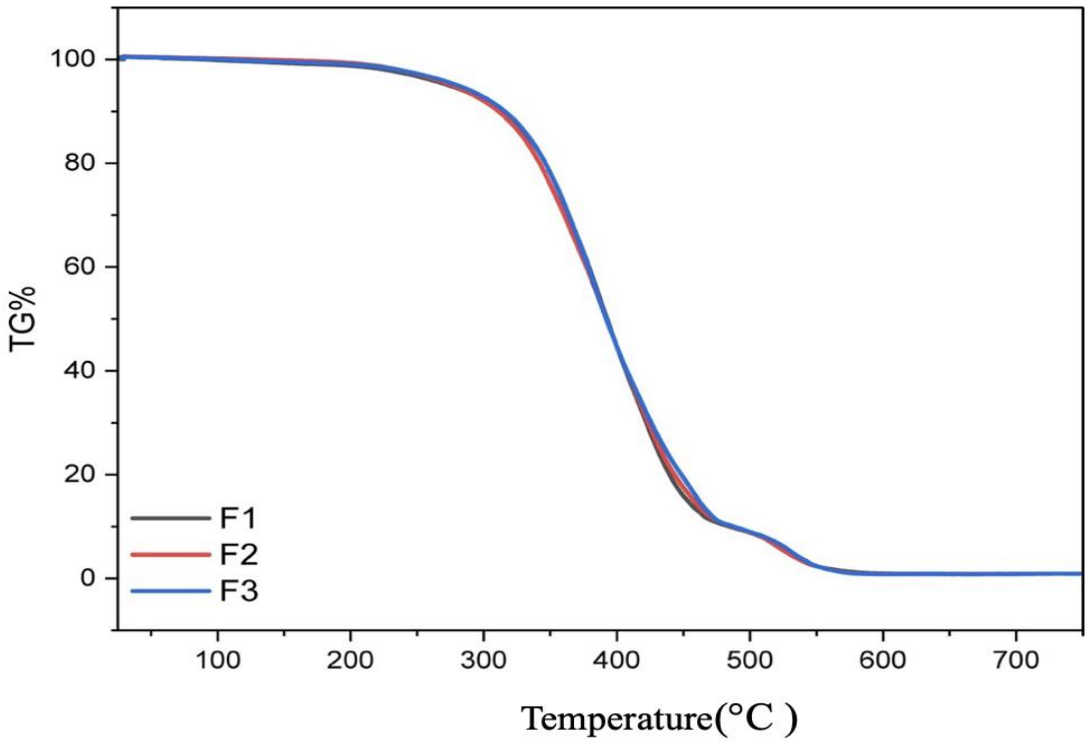


Figure 4.8. TG-DTA thermogram of prepared films

4.5.3. Gel content of prepared films

UV-cured films prepared by applying thiol-ene click chemistry were kept in an oven at 120 °C for 1 hour and another 24 hours, and extra post-cure was applied. Gel content measurements were taken to compare the cross-link properties of the films cured only in UV and the films that were applied extra post-cure after UV treatment. A piece was cut from each sample and its weight was measured, and then the samples were kept in acetone for 24 hours. At the end of this period, the weight of the free films was measured again and the gel content percentage was calculated. The following formula was used to calculate gel content percentage.

$$\% \text{ Gel Content} = \frac{m_1}{m_2} \text{ x } 100$$

m1: First weighing mass (g)

m2: Final weighing mass (g)

Table 4.3. Gel content analysis of the film in different formulations at different thermal times

SAMPLE	CALCULATED GEL CONTENT(%)
F1- UV	72.63
F1- UV + 1h	83.42
F1- UV + 24h	96.28
F2- UV	69.02
F2- UV + 1h	84.56
F2- UV + 24h	95.28
F3- UV	73.14
F3- UV + 1h	85.6
F3- UV + 24h	95.82

A comparison of gel content percentages is given in the table numbered Table 4.3 above. This result confirms the high rate of cross-link formation. With heating the thioester in the dynamic bond opens and they participate in the cross-linking reaction. Thus, when we evaluated each formulation on its own, it was seen that the percentage gel content increased with increasing thermal cure. This shows that the thiol-ene reaction with acrylates with the SH functional structure was successful.

Thiol-cured systems exhibit heightened functional group conversion attributed to a delayed gel point. Meanwhile, it is widely acknowledged that a gel content of around 95% indicates that the coatings have fully cured. Hence, gel content values ranging from 92% to 97% in the cured films validate the establishment of a densely cross-linked network within the coating system [84].

4.5.4. Tensile test of prepared film

The elongation at break percentages of the films prepared with the tensile rupture test are given in table 7.1.7 below and their mechanical properties are compared. Each test was repeated four times and the test result closest to the mean was obtained. When the table is examined, an increase in breaking strain and Young modulus (E) was observed after the final curing at 120 °C applied after UV curing. However, it was still a low-modulus material and the average elongation at break was around 20%. Low modulus shows us

that it is a weak material. Since it is an oil-based material, the elongation at break was expected to be around 20%.

Table 4.4. Tensile test analysis of prepared film

SAMPLE	E Module (N/mm^2)	Breaking Strength (kg /cm^2)	Breaking Strain (%)
F1- UV	0.3	0,59	20,44
F1- UV + 1h	0.71	3.04	28.43
F1- UV + 24h	1.09	11.16	30.64
F2- UV	0.48	0.92	15.42
F2- UV + 1h	1.61	2.01	17.3
F2- UV + 24h	1.13	5.3	26.47
F3 -UV	0.15	0.8	20.15
F3 -UV + 1h	0.22	1.27	17.71
F3- UV + 24h	0.31	6.49	27.4

4.6. Physical and Mechanical Performance Properties of Coatings

4.6.1. Pendulum hardness test analysis

Coatings were prepared on micro-glass surfaces with the determined formulations. Hardness analysis tests were performed on these coatings and the results in Table 4.5 below were obtained.

Table 4.5. Hardness test analysis of coatigs were prepared on microglass

SAMPLE	HARDNESS (s)
F1	14 ,6
F1-UV+1h	20
F1-UV+24h	47.6
F2-UV	17
F2-UV+1h	21.6
F2-UV+24h	62.6
F3-UV	16.6
F3-UV+1h	17.6
F3-UV+24h	49

According to these results (Table 4.5), during the post-cure application applied at 120 degrees to coatings increased the hardness, the cross-linking rate increased with curing and, extra curing created more crosslinks. As a result of it, physically harder coatings were obtained. F1, F2, and F3 samples hardness are close and comparable to one another.

4.6.2. Pencil hardness

As seen in table 12 below due to the scratch resistance provided by the long aliphatic chains of vegetable oil derivatives, all coatings possess a hardness rating of 7H+ against scratching.

Table 4.6. Hardness test analysis of coatigs on microglass

SAMPLE	PENCIL HARDNESS
F1	7H+
F1-UV+1h	7H+
F1-UV+24h	7H+
F2-UV	7H+
F2-UV+1h	7H+
F2-UV+24h	7H+
F3-UV	7H+
F3-UV+1h	7H+
F3-UV+24h	7H+

4.6.3. Contact Angle

Contact angle measurements were carried out to examine the superhydrophobic properties of the prepared coatings. The test result is the average of 3 measurements.

Table 4.7. Water contact angle values of coatings

SAMPLE	CA LEFT
F1-UV	82.37
F2-UV	84.97
F3-UV	91.1

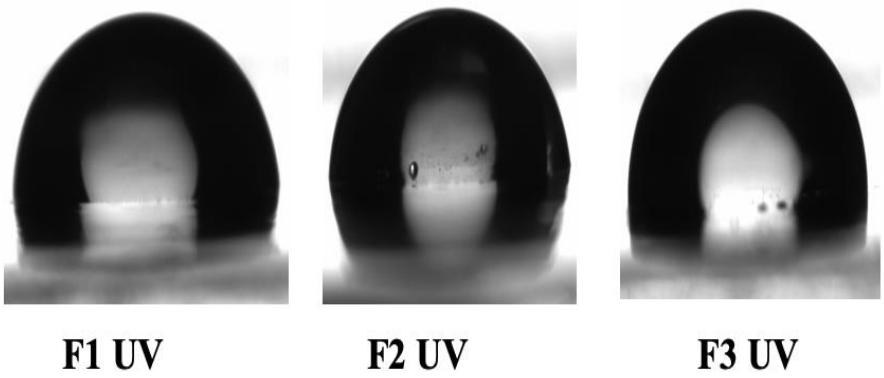


Figure 4.9. Images of coatings water contact angle

There is a cross-linked molecule consisting of AELO and a thiol compound synthesized in the F1 Formulation. In the F2 and F3 formulations, cross-linking was made by adding an increasing amount of PETMP in addition to this F1 formulation. As a result, it was observed that the structure became more hydrophobic as PETMP increased. This small increase may be due to the difference in PETMP.

4.6.4. Cross-Cut analysis

In images of cross-cut test analyses, the score is 0 according to ISO standards. This shows that adhesion resistance is strong.

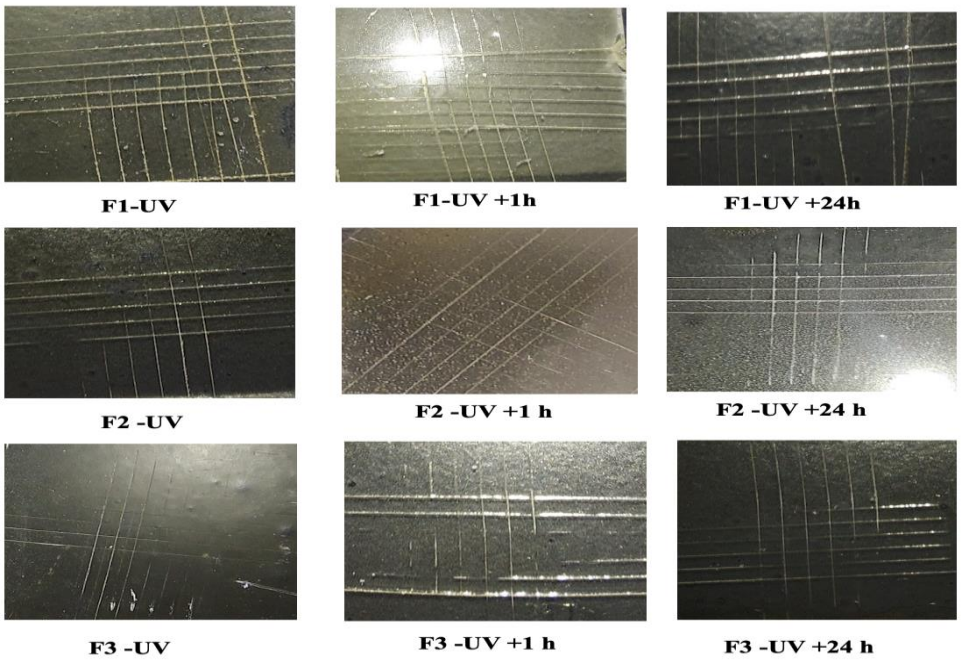


Figure 4.10. Adhesion test images of coatings

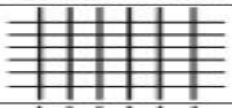
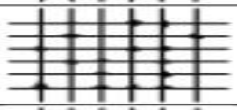
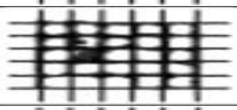
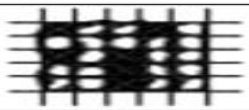
Score	Appearance of surface of cross-cut area from which flaking has occurred
0	
1	
2	
3	
4	
5	

Figure 4.11. Scoring of cross-cut test results [85].

RESULTS

This thesis' primary goal is to provide less costly, renewable, and ecologically friendly substitute formulations for thiol-acrylate-based UV curable coatings rather than using raw ingredients generated from petroleum. For this purpose, firstly, flaxseed was used as a more environmentally friendly vegetable oil instead of petroleum-based products. The reason for using this oil is that it has the highest unsaturated C=C double bond content among other vegetable oils. This feature gives it an advantage in terms of chemical reactivity. Since vegetable oils have active sites that can be functionalized with the right procedures, the double bonds in the oil chain can be subjected to epoxidation, acrylation and thiol-ene bonding processes to create a renewable monomer. In this study, linseed oil was first epoxidized. Firstly, the oxirane value of epoxidized linseed oil was found. The oxirane value was 7.9%, which is accepted as a good value in the literature. Structural characterization of ELO was performed by FTIR spectroscopy. Upon analyzing the FTIR spectrum of ELO, the carbon-carbon double bond characteristic of flaxseed oil, typically observed at 1654 cm^{-1},, is nearly absent in ELO, signifying the disruption of these double bonds due to epoxidation. The presence of a peak at 822.08 cm^{-1}, provides evidence of the epoxidation process, denoting the cleavage of the double bonds and the formation of C-O-C stretching attributable to the oxirane ring.

Then, the synthesized ELO was acrylated with the acrylation reaction and AELO was synthesized. The purpose of the acrylation process is to chemically improve epoxidized vegetable oils and create more value-added products. Structural characterization of the synthesized AELO was determined by FTIR and H-NMR spectroscopy. In the analysis of the FTIR Spectrum, the presence of a peak at 1719.19 cm^{-1}, indicates the C=O stretching associated with the carbonyl group. The stretching vibrations of the vinyl group (-CH=CH2) in the acrylate are identified at peaks situated at 812 cm^{-1}, 984 cm^{-1}, and 1408 cm-1. Moreover, the peak at 1633 cm^{-1}, is attributed to the functional group involving the C=C stretch. Consequently, it was noted that the peaks corresponding to the epoxy group were no longer present following the acrylation procedure. At the same time, the acrylate group peaks occurring between 5.6 and 6.4 ppm in the NMR spectrum prove the accuracy of the structure.

When we examine the structural characterization of thiol synthesis, the disappearance of the peak at 1854 cm^{-1}, of the maleic anhydride during the thiol synthesis shows that the anhydride ring is opened and thiol synthesis has taken place. The peak manifesting at 2568 cm^{-1}, (S-H) is attributed to thiol groups, corroborating the synthesis of thiols. Also in the NMR spectrum, the main peak shows that the thiol molecule is synthesized successfully seen in 1.33 ppm.

Tg values of the prepared films were determined by DSC. According to the results examined, the glass transition temperatures (Tg) of films containing -SH group cross-linked with UV light were determined as 11.31, 7.1 and 1.9 °C, respectively. As the amount of pentaerythritol tetrakis (4SH) monomer added to the film composition increased, the aliphatic flexible chains resulting from this monomer decreased the Tg value. While it was expected that cross-linking and therefore Tg would increase with the increase in -SH content, the decrease in Tg had a more dominant effect, thanks to the flexibility of the aliphatic chains. After UV curing, the cross-link density increased in the samples exposed to thermal curing and, accordingly, the Tg value increased. As previous research has shown, the presence of free thiols in the reaction medium can promote thiol-thioester exchange, increasing cross-linking and ultimately leading to the creation of stress-reduction networks that are more effective.

TGA analysis was performed to determine the thermal stability of the films. According to the thermogram profiles, the main degradation process of the films begins at approximately 273°C. With the increase of -SH content, the initial degradation temperature of the films increases up to 280 °C. In the F1 film without PETMP, the maximum mass loss occurred at 90% and at 484°C, while in the F3 film containing PETMP, this value was determined as 487°C. These findings show that the films are resistant to high temperatures and that the actual degradation occurs above 300°C. Therefore, these films are predicted to be safe and suitable for a variety of coating applications.

When the analysis for the percentage of gel content was examined, it was seen that the percentage of gel content increased with increasing thermal postcure for each formulation, and this value increased to an average of 95%. This shows that the thiol-ene reaction with acrylates having the SH functional structure is successful.

When the tensile-rupture test results of the films are examined, it is seen that it is a low modulus material and the average elongation at break is around 20%. It is understood that this situation is due to the flexibility in the structure of the plant content.

Upon conducting hardness and pencil test analyses on the coatings, it was observed that all films exhibited a value 7H+ in the pencil test. Additionally, in the hardness analysis, each film formulation demonstrated a harder material when considered individually, attributed to the additional post-cure application which resulted in enhanced cross-linking, thereby rendering the material harder. In the cross-cut analysis, the value was found to be 0 according to ISO standards. This shows that the adhesion resistance is high.

Finally, vegetable oil-based coatings prepared using UV-induced thiol-ene click chemistry are considered a sustainable and environmentally friendly alternative to petroleum-derived materials in a wide range of usage areas, and are also expected to provide significant benefits to the industry.

REFERENCES

[1] Lligadas, G., Ronda, J. C., Galià, M., & Cádiz, V. (2013). Renewable polymeric materials from vegetable oils: a perspective. Materials Today, 16(9), 337–343. doi:10.1016/j.mattod.2013.08.

[2] Monroe, K., Kirk, T., Hull, V., Biswas, E., Murawski, A., & Quirino, R. L. (2019). Vegetable Oil-Based Polymeric Materials: Synthesis, Properties, and Applications. Reference Module in Materials Science and Materials Engineering. doi:10.1016/b978-0-12-803581-8.11521-8

[3] Miao, S., Wang, P., Su, Z., & Zhang, S. (2014). Vegetable-oil-based polymers as future polymeric biomaterials. Acta Biomaterialia, 10(4), 1692–1704. doi:10.1016/j.actbio.2013.08.0

[4] Murawski, A., & Quirino, R. L. (2018). Vegetable Oils as a Chemical Platform. Gels Horizons: From Science to Smart Materials, 125–152. doi:10.1007/978-981-10-6080-9_6

[5] https://www.reportlinker.com/p087311/World-Vegetable-Oils-Markets.html

[6] Karak, N. (2012). Vegetable oils and their derivatives. Vegetable Oil-Based Polymers, 54-95. doi:10.1533/9780857097149.54

[7] Ataei, S., Khorasani, S. N., & Neisiany, R. E. (2019). Biofriendly vegetable oil healing agents used for developing self-healing coatings: A review. Progress in Organic Coatings, 129, 77–95. doi:10.1016/j.porgcoat.2019.01

[8] Karmakar, G., Ghosh, P., & Sharma, B. (2017). Chemically Modifying Vegetable Oils to Prepare Green Lubricants. Lubricants, 5(4), 44. doi:10.3390/lubricants5040044

[9] Vegetable oils as monomeric and polymeric materials: A graphical review Caroline Gaglieri a , Rafael T. Alarcon b , Aniele de Moura a

[10] https://www.osti.gov/etdeweb/servlets/purl/21512209

[11] Seniha Güner, F., Yağcı, Y., & Tuncer Erciyes, A. (2006). Polymers from triglyceride oils. Progress in Polymer Science, 31(7), 633–670. doi:10.1016/j.progpolymsci.2001

[12] Zhang, C., Garrison, T. F., Madbouly, S. A., & Kessler, M. R. (2017). Recent advances in vegetable oil-based polymers and their composites. Progress in Polymer Science, 71, 91–143. doi:10.1016/j.progpolymsci.2016.12.009

[13] Mosiewicki, M. A., & Aranguren, M. I. (2015). Recent developments in plant oil based functional materials. Polymer International, 65(1), 28–38. doi:10.1002/pi.5033

[14] Adekunle, K.F. (2015) A Review of Vegetable Oil-Based Polymers: Synthesis and Applications. Open Journal of Polymer Chemistry, 5, 34-40. http://dx.doi.org/10.4236/ojpchem.2015.53004

[15] Lu, Y., & Larock, R. C. (2009). Novel Polymeric Materials from Vegetable Oils and Vinyl Monomers: Preparation, Properties, and Applications. Chem Sus Chem, 2(2), 136–147. doi:10.1002/cssc.200800241

[16] Vilela, C. A. C. (2012). Synthesis of new vegetable oil-based polymeric materials, Phd Thesis, Universidade de Aveiro.

[17] Xia, Y., & Larock, R. C. (2010). Vegetable oil-based polymeric materials: synthesis, properties, and applications. Green Chemistry, 12(11), 1893. doi:10.1039/c0gc00264j

[18] Sung, J. (2018). Design and synthesis of plant oil-based UV-curable acrylates for sustainable coating applications, Phd Thesis, Kansas State University

[19] Goyal, A., Sharma, V., Upadhyay, N., Gill, S., & Sihag, M. (2014). Flax and flaxseed oil: an ancient medicine & modern functional food. Journal of Food Science and Technology, 51(9), 1633–1653. doi:10.1007/s13197-013-1247-9

[20] Patterson, H. B. W. (2011). Hydrogenation Methods. Hydrogenation of Fats and Oils, 189–278. doi:10.1016/b978-1-893997-93-6.50014-2

[21] Su, Y., Zhang, S., Chen, Y., Yuan, T., & Yang, Z. (2020). One-step synthesis of novel renewable multi-functional linseed oil-based acrylate prepolymers and its application in UV-curable coatings. Progress in Organic Coatings, 148, 105820. doi:10.1016/j.porgcoat.2020.10

[22] Kuroda, A., Joly, P., Shibata, N., Takeshige, H., & Asakura, K. (2008). An organic–inorganic hybrid composite as a coating agent. Journal of the American Oil Chemists' Society, 85(6), 549-553. https://doi.org/10.1007/s11746-008-1230-1

[23] Mosiewicki, M., Rojas, Ó., Sibaja, M., Borrajo, J., & Aranguren, M. (2007). Aging study of linseed oil resin/styrene thermosets and their composites with wood flour. Polymer International, 56(7), 875-881. https://doi.org/10.1002/pi.2218-

[24] Franco, Martins, López-Pedrouso, Purriños, Cerqueira, Vicente, Lorenzo. (2019). Strategy towards Replacing Pork Backfat with a Linseed Oleogel in Frankfurter Sausages and its Evaluation on Physicochemical, Nutritional, and Sensory Characteristics. Foods, 8(9), 366. doi:10.3390/foods8090366

[25] https://www.gminsights.com/industry-analysis/linseed-oil-market

[26] Kolář, M., Machotová, J., Hájek, M., Honzíček, J., Hájek, T., & Podzimek, Š. (2023). Application of Vegetable Oil-Based Monomers in the Synthesis of Acrylic Latexes via Emulsion Polymerization. Coatings, 13(2), 262; https://doi.org/10.3390/coatings13020262

[27] Musik, M., Bartkowiak, M., & Milchert, E. (2021). Advanced methods for hydroxylation of vegetable oils, unsaturated fatty acids and their alkyl esters. Coatings, 12(1), 13. https://doi.org/10.3390/coatings12010013

[28] Samarth, N.B. and Mahanwar, P.A. (2015) Modified Vegetable Oil Based Additives as a Future Po- lymeric Material—Review. Open Journal of Organic Polymer Materials, 5, 1-22. http://dx.doi.org/10.4236/ojopm.2015.51001

[29] Hernandez, B. S. (2016). Thermosetting polymers from renewable, Phd Thesis, Auburn University

[30] Kalkandelen, M. (2019). Epoxidation of soybean oil over mesoporous titanium and niobium incorporated SBA-15 catalysts, Phd Thesis, Izmir Institute of Technology, Turkey

[31] Espinoza-Perez, J. D. (2010). Production, characterization, and raw material cost analysis of a canola oil-epoxy resin applied to composites, Phd Thesis, North Dakota State University.

[32] Saurabh, T., Patnaik, M., Bhagt, S. L., & Renge, V. C. (2011). Epoxidation of vegetable oils: a review. Int. J. Adv. Eng. Technol, 2(4), 491-501.

[33] World Journal of Analytical Chemistry. 2022, 7(1), 1-6. DOI: 10.12691/wjac-7-1-1 Received July 28, 2022; Revised September 05, 2022; Accepted September 14, 202 World Journal of Analytical Chemistry, 2022, Vol. 7, No. 1, 1.

[34] Turco, R., Tesser, R., Russo, V., Cogliano, T., Di Serio, M., & Santacesaria, E. (2021). Epoxidation of linseed oil by performic acid produced in situ. Industrial & Engineering Chemistry Research, 60(46), 16607-16618.

[35] Schwaiger, M. and Resch-Fauster, K. (2022). Mechanical flexible epoxy resins with 100% bio-based carbon content based on epoxidized vegetable oils. Journal of Applied Polymer Science, 139(48). https://doi.org/10.1002/app.53233

[36] Milchert, E., Malarczyk, K., & Kłos, M. (2015). Technological aspects of chemoenzymatic epoxidation of fatty acids, fatty acid esters and vegetable oils: a review. Molecules, 20(12), 21481-21493. https://doi.org/10.3390/molecules201219778

[37] Hosney, H., Nadiem, B., Ashour, I., Mustafa, I., & El-Shibiny, A. (2018). Epoxidized vegetable oil and bio-based materials as pvc plasticizer. Journal of Applied Polymer Science, 135(20). https://doi.org/10.1002/app.46270

[38] Chandrasekara, G., Mahanama, M. K., Edirisinghe, D. G., & Karunanayake, L. (2011). Epoxidized vegetable oils as processing aids and activators in carbon-black filled natural rubber compounds. Journal of the National Science Foundation of Sri Lanka, 39(3), 243. https://doi.org/10.4038/jnsfsr.v39i3.3628

[39] Azmi, I. S., Kadir, M. Z. A., Sharif, N. A., Raofuddin, D. N. A., & Jalil, M. J. (2023). A novel approach for sunflower oil based polyol production by ring opening of epoxidized linoleic acid. Journal of Elastomers &Amp; Plastics, 55(4), 626-638. https://doi.org/10.1177/00952443231165415

[40] Ecochard, Y., Auvergne, R., Boutevin, B., & Caillol, S. (2019). Linseed oil-based thermosets by Aza-Michael polymerization. European Journal of Lipid Science and Technology. doi:10.1002/ejlt.201900145

[41] Ho, Y. H., Parthiban, A., Thian, M. C., Ban, Z. H., & Siwayanan, P. (2022). Acrylated biopolymers derived via epoxidation and subsequent acrylation of vegetable oils. International Journal of Polymer Science, 2022, 1-12. https://doi.org/10.1155/2022/6210128

[42] Grishchuk, S., Leanza, R., Kirchner, P., & Karger-Kocsis, J. (2011). “Greening” of unsaturated polyester resin based bulk molding compound with acrylated epoxidized soybean and linseed oils: effect of urethane hybridization. Journal of Reinforced Plastics and Composites, 30(17), 1455–1466. DOI:10.1177/0731684411421541

[43] Habib, F., & Bajpai, M. (2011). Synthesis and characterization of acrylated epoxidized soybean oil for UV cured coatings.

[44] Briede, S., Jurinovs, M., Nechausov, S., Platnieks, O., & Gaidukovs, S. (2022). State-of-the-art uv-assisted 3d printing via a rapid syringe-extrusion approach for photoactive vegetable oil acrylates produced in one-step synthesis. Molecular Systems Design & Engineering, 7(11), 1434-1448. https://doi.org/10.1039/d2me00085g

[45] Soucek, M. D., & Ren, X. (2015). UV-curable coating technologies. *Photocured materials*, 15-48. doi:10.1039/9781782620075-00015

[46] Tong, J., Xie, S., Miao, J. T., Luo, J., & Liu, R. (2024). Preparation of UV-cured polyurethane-urea acrylate coatings with high hardness and toughness. *Progress in Organic Coatings*, *186*, 107969.

[47] Cheng, F., Fan, Y., He, N., Song, Y., Shen, J., Gong, Z., & Yang, X. (2022). Castor oil based high transparent UV cured silicone modified polyurethane acrylate coatings with outstanding tensile strength and good chemical resistance. *Progress in Organic Coatings*, *163*, 106624. https://doi.org/10.1016/j.porgcoat.2021.106624

[48] Hu, Y., Jia, P., Shang, Q., Zhang, M., Feng, G., Liu, C., & Zhou, Y. (2019). Synthesis and application of UV-curable phosphorous-containing acrylated epoxidized soybean oil-based resins. *Journal of Bioresources and Bioproducts*, *4*(3), 183-191.

[49] Jiao, X., Song, Y., He, N., Wang, X., Huang, M., Zhang, L., & Yang, X. (2022). High Tensile Strength UV-Cured Castor Oil-Based Silicone-Modified Polyurethane Acrylates. *ACS omega*, *7*(15), 12680-12689.

[50] Rengasamy, S., & Mannari, V. (2013). Development of soy-based UV-curable acrylate oligomers and study of their film properties. *Progress in Organic Coatings*, *76*(1), 78-85. doi:10.1016/j.porgcoat.2012.08

[51] Ilgun, K. (2014) Karbon nanotüp içeren UV ışınlarıyla kürlenmiş nanokompozit kaplamalar, Master's Thesis,Marmara University, Institute of Science and Technology, Turkey.

[52] Kartal, I. (2009). UV ile sertleşebilen çizilmeye, aşınmaya ve kirlenmeye dayanıklı kaplama malzemeleri ve uygulamaları,Phd Thesis, Marmara University , Institute of Science and Technology, Turkey.

[53] Baştürk, E.(2018) Isıl enerji depolama kapasitesine sahip UV ışınlarıyla sertleşebilen kompozit yapıların geliştirilmesi,Phd Thesis, Marmara University , Institute of Science and Technology, Turkey.

[54] Nguyen, T. V., Do, T. V., Ngo, T. D., Nguyen, T. A., Vu, Q. T., & Thi, L. P. (2022). Photocurable acrylate epoxy/ZnO–Ag nanocomposite coating: fabrication, mechanical and antibacterial properties. *RSC advances*, *12*(36), 23346-23355.

[55] Qianhe, W. (2016). Acrylated alkyds, PHD Thesis, Akron University.

[56] Tezel, Ö. (2019) Kendi kendini onarabilen UV ışınları ile kuruyabilen kaplamaların hazırlanması ve performans özelliklerinin incelenmesi, Master's Degree , Marmara University , Institute of Science and Technology, Turkey.

[57 Mülazim, Y. (2011) UV ışınlarıyla sertleşebilen hidrofobik ve oleofobik kaplamaların geliştirilmesi ve karakterizasyonu, Phd Thesis, Marmara University , Institute of Science and Technology, Turkey.

[58] Schwalm, R. (2007). *Raw Materials. UV Coatings, 94–139.* doi:10.1016/b978-044452979-4/50004-4

[59] Çınar, M. (2016) UV ile kürlenebilen siloksan bazlı yeni kaplama malzemelerinin sentezi ve karakterizasyonu, Master's Thesis, Marmara University , Institute of Science and Technology, Turkey.

[60] Su, Y., Zhang, S., Zhou, X., Yang, Z., & Yuan, T. (2020). A novel multi-functional bio-based reactive diluent derived from cardanol for high bio-content UV-curable coatings application. Progress in Organic Coatings, 148, 105880. doi:10.1016/j.porgcoat.2020.10

[61] Huang, J., Xiong, Y., Zhou, X., Yang, Z., & Yuan, T. (2022). A novel polyfunctional polyurethane acrylate prepolymer derived from bio-based polyols for UV-curable coatings applications. *Polymer Testing*, *106*, 107439.

[62] Zhou, Y., & Qu, J. (2023). Preparation of low viscosity and high flexibility epoxy acrylate and its application in UV-curable coatings. *Journal of Coatings Technology and Research*, 1-10.

[63] Yan, R., Yang, D., Zhang, N., Zhao, Q., Liu, B., Xiang, W., Hu, W. (2018). Performance of UV curable lignin based epoxy acrylate coatings. Progress in Organic Coatings, 116, 83–89. doi:10.1016/j.porgcoat.2017.11.

[64] Hu, Y., Shang, Q., Bo, C., Jia, P., Feng, G., Zhang, F., Zhou, Y. (2019). *Synthesis and Properties of UV-Curable Polyfunctional Polyurethane Acrylate Resins from Cardanol. ACS Omega, 4(7), 12505–12511*

[65] Liu, R., Luo, J., Ariyasivam, S., Liu, X., & Chen, Z. (2017). High biocontent natural plant oil based UV-curable branched oligomers. Progress in Organic Coatings, 105, 143–148. doi:10.1016/j.porgcoat.2016.11

[66] Bozdağ, B.(2019) Preparation of antibacterial, UV curable coatings and investigation of performance properties, Master's Thesis, Marmara University , Institute of Science and Technology, Turkey.

[67] Hoogenboom, R. (2023). Click chemistry in polymer science. Chem, 9(9), 2416-2424.

[68] Huang, D., Liu, Y., Qin, A., & Tang, B. Z. (2018). Recent advances in alkyne-based click polymerizations. Polymer Chemistry, 9(21), 2853–2867. doi:10.1039/c7py02047c

[69] Güneş, İ. (2023). Biyobazlı kendiliğinden çapraz bağlanabilen fonksiyonel polimerik malzemelerin geliştirilmesi.

[70] Tremblay-Parrado, K. K., García-Astrain, C., & Avérous, L. (2021). Click chemistry for the synthesis of biobased polymers and networks derived from vegetable oils. *Green Chemistry*, *23*(12), 4296-4327.

[71] Arslan, M., Acik, G., & Tasdelen, M. A. (2019). The emerging applications of click chemistry reactions in the modification of industrial polymers. Polymer Chemistry, 10(28), 3806–3821. doi:10.1039/c9py00510b

[72] Pezzana, L., & Sangermano, M. (2021). Fully biobased UV-cured thiol-ene coatings. Progress in Organic Coatings, 157, 106295. doi:10.1016/j.porgcoat.2021.10

[73] Uygun, M., (2010). Influence of type of initiation on thiol–ene "click" chemistry. *Macromolecular Chemistry and Physics*,

[74] Ge, M., Miao, J.-T., Zhang, K., Wu, Y., Zheng, L., & Wu, L. (2020). Building Biobased, Degradable, Flexible Polymer Networks from Vanillin via Thiol-Ene "Click" Photopolymerization. Polymer Chemistry. doi:10.1039/d0py01407a

[75] L ligadas, G., Ronda, J. C., Galià, M., & Cádiz, V. (2013). Monomers and polymers from plant oils via click chemistry reactions. Journal of Polymer Science Part A: Polymer Chemistry, 51(10), 2111–2124. doi:10.1002/pola.26620

[76] Resetco, C., Hendriks, B., Badi, N., & Du Prez, F. (2017). Thiol–ene chemistry for polymer coatings and surface modification–building in sustainability and performance. *Materials Horizons*, *4*(6), 1041-1053.

[77] Wendeln, C., Rinnen, S., Schulz, C., Arlinghaus, H. F., & Ravoo, B. J. (2010). Photochemical Microcontact Printing by Thiol−Ene and Thiol−Yne Click Chemistry. Langmuir, 26(20), 15966–15971. doi:10.1021/la102966j

[78] Black, M. R., Rawlings,J.W.(2009). Thiol–ene UV-curable coatings using vegetable oil macromonomers. *Europen Polymer Journal, 45(5), 1433-1441*.

[79] Altıntaş, Z. (2012) Termoplastik poliüretanın sentezi ve kompozit hazırlama uygulamaları. Phd Thesis, Marmara University, Turkey.

[80] Lligadas, G., Ronda, J. C., Galià, M., & Cádiz, V. (2010). Plant oils as platform chemicals for polyurethane synthesis: current state-of-the-art. Biomacromolecules, 11(11), 2825-2835. https://doi.org/10.1021/bm100839x

[81] Rana, A., & Evitts, R. W. (2015). Synthesis and characterization of acrylated epoxidized flaxseed oil for biopolymeric applications. *International Polymer Processing*, *30*(3), 331-336.

[82] Díez-Pascual, A. M., & Díez-Vicente, A. L. (2015). Development of linseed oil–TiO 2 green nanocomposites as antimicrobial coatings. *Journal of Materials Chemistry B*, *3*(21), 4458-4471.

[83] Podgórski, M., Mavila, S., Huang, S., Spurgin, N., Sinha, J., & Bowman, C. N. (2020). Thiol–Anhydride dynamic reversible networks. *Angewandte Chemie International Edition*, *59*(24), 9345-9349.

[84] Mishra, V., Desai, J., & Patel, K. I. (2017). High-performance waterborne UV-curable polyurethane dispersion based on thiol–acrylate/thiol–epoxy hybrid networks. *Journal of Coatings Technology and Research*, *14*(5), 1069-1081

[85] Murdan, S., Kerai, L., & Hossin, B. (2015). To what extent do in vitro tests correctly predict the in vivo residence of nail lacquers on the nail plate?. *Journal of Drug Delivery Science and Technology*, *25*, 23-28.

[86] Çakmakçı, E., Mülazim, Y., Kahraman, M. V., & Apohan, N. K. (2012). Preparation and characterization of boron containing thiol–ene photocured hybrid coatings. *Progress in Organic Coatings*, *75*(1-2), 28-32.

[87] He, Y., Huang, J., He, J., & Xu, Z. (2018). Synthesis of a thiol building block for the crystallization of a semiconducting gyroidal metal-sulfur framework. *JoVE (Journal of Visualized Experiments)*, (134), e57455

[88] Bowman, C. N., Podgórski, M., Mavila, S., Huang, S., Spurgin, N., & Sinha, J. (2020). Thiol-Anhydride Dynamic Reversible Networks. Angewandte Chemie International Edition. doi:10.1002/anie.202001388

[89] Finnveden, M., Nameer, S., Johansson, M., & Martinelle, M. (2016). One-component thiol-alkene functional oligoester resins utilizing lipase catalysis. *Macromolecular Chemistry and Physics*, *217*(12), 1335-1341.

ADDITIONAL RESOURCES

Figure 1

FTIR Spectra of F2 Formulation Films

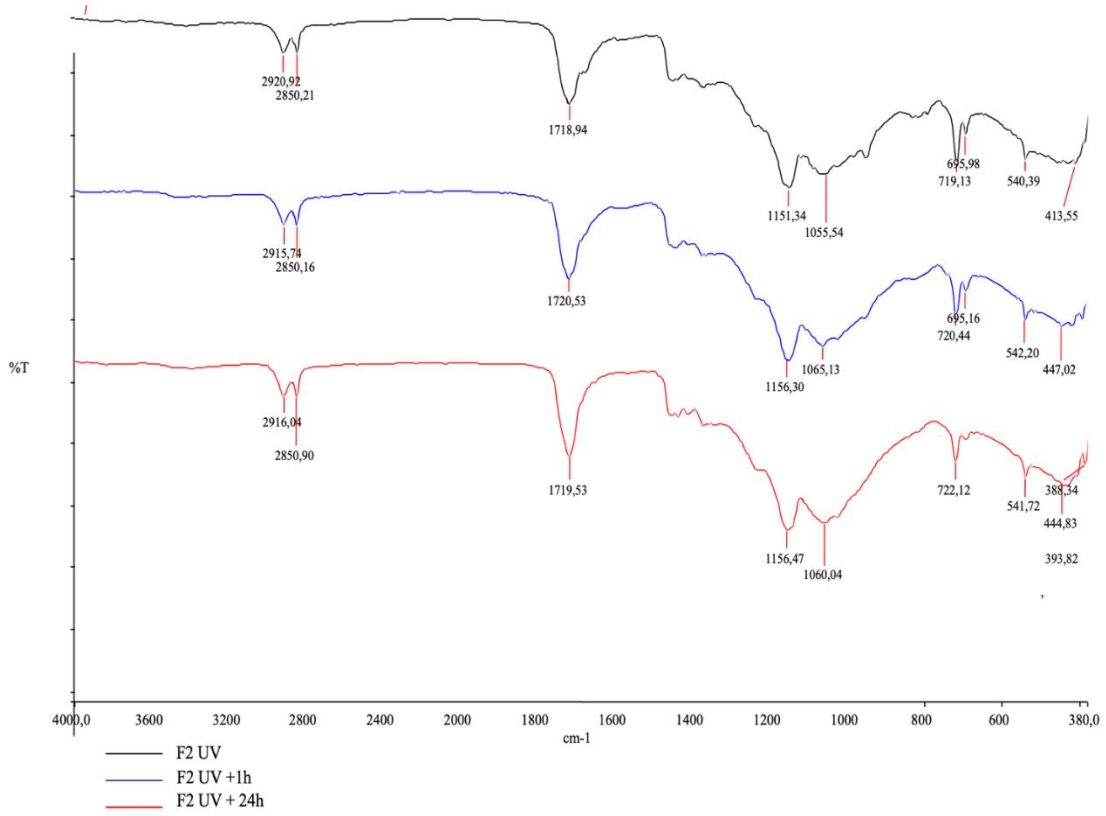


Figure 2

FTIR Spectra of F3 Formulation Films

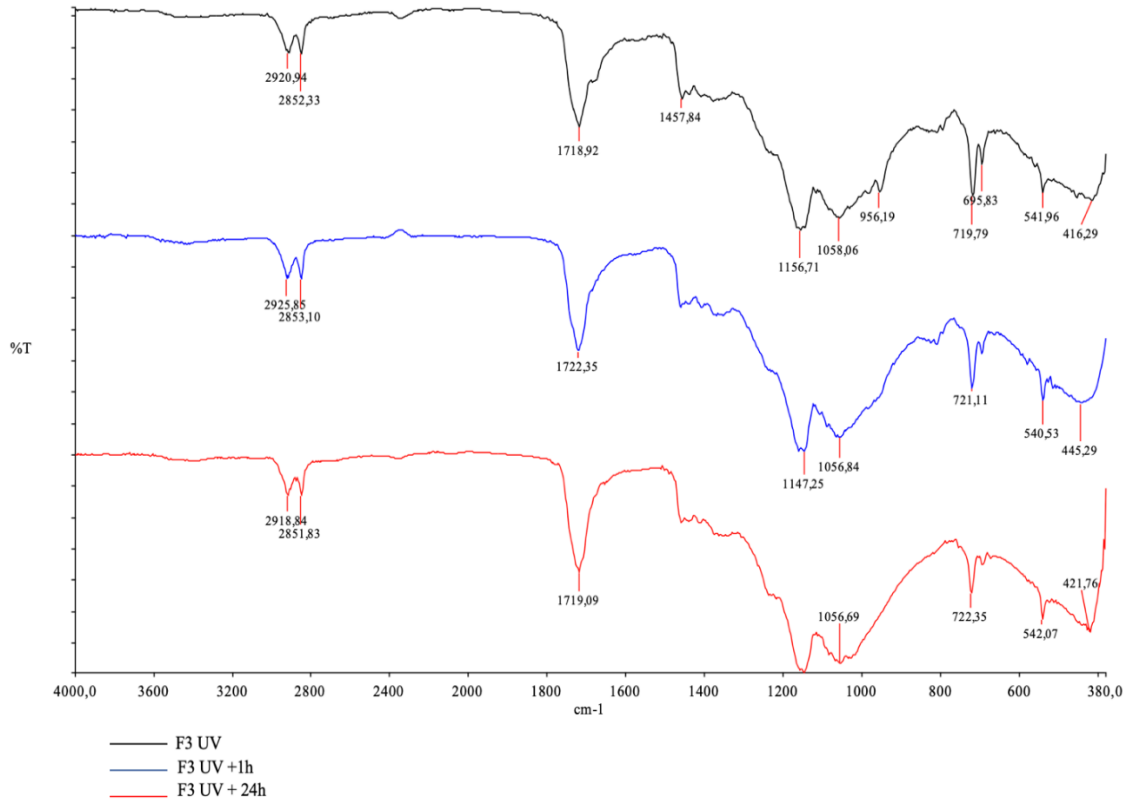


Figure 3

DSC analysis results of prepared F1formulations

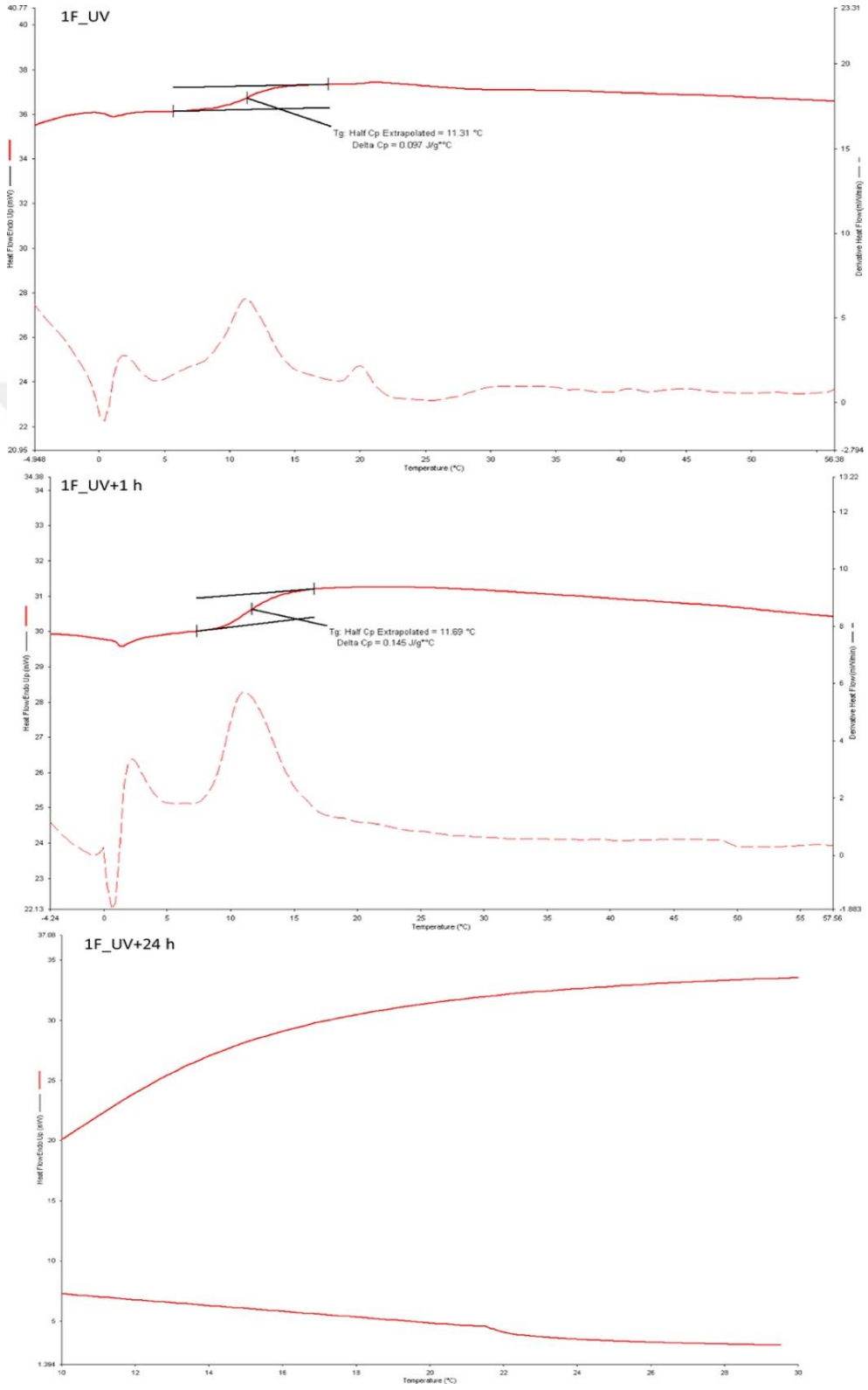
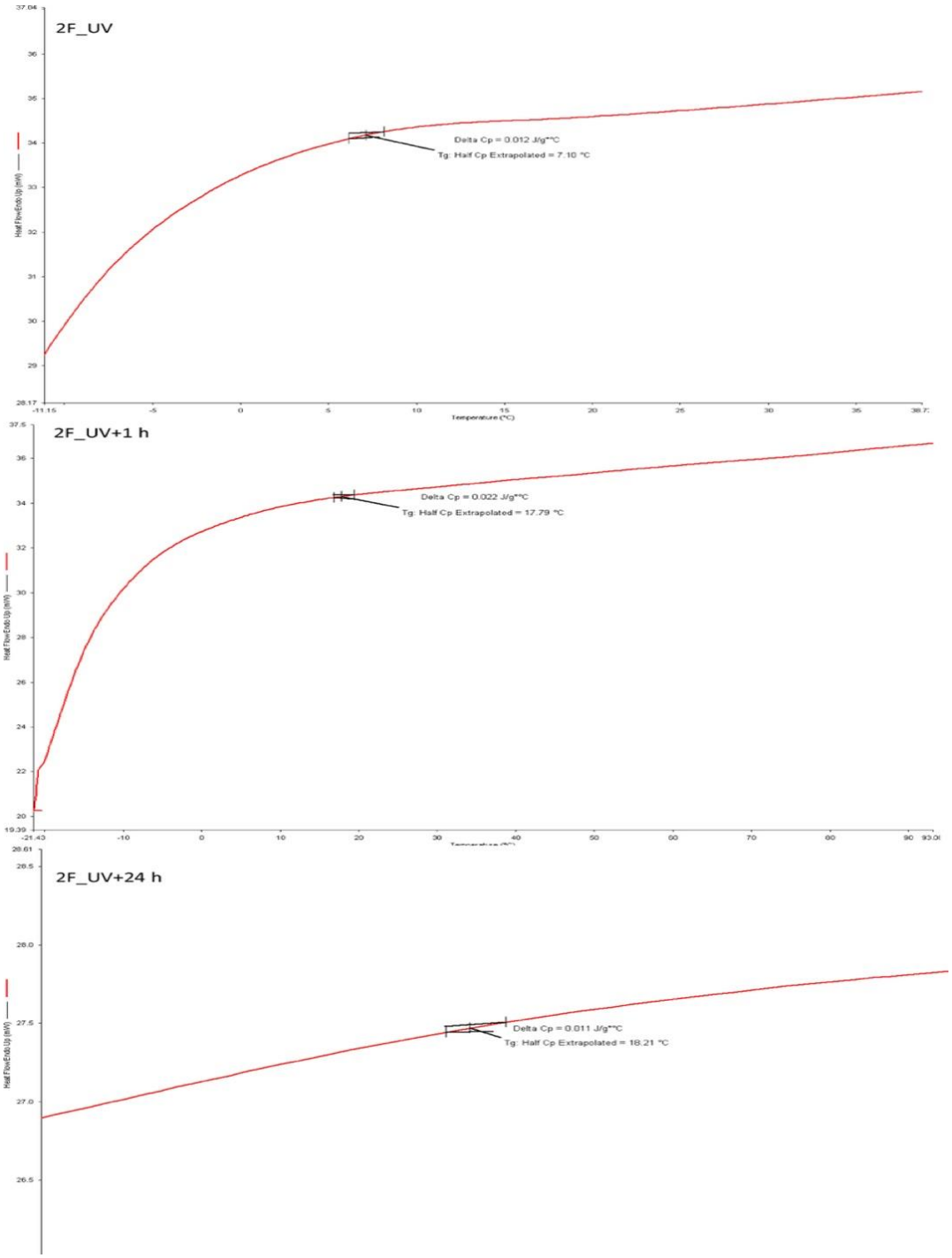


Figure 4

DSC analysis results of prepared F2 formulations



RESUME

Eda Gaş. She graduated from Marmara University, Department of Chemistry in 2020 and then started her master's degree in Polymer Science and Technology at Marmara University. She worked as a sales specialist at Prosim Kimya Company between January 2021 and November 2021. Later, she started working as a sales specialist at Ege Kimya company in 2023.

Congresses Attended

1. 9th International Conference on Materials Science and Nanotechnology for Next Generation, Preparation of Vegetable Oil-Based Composite Coatings by UV Induced Thiol- Ene Click Chemistry and Investigation of Their Properties, Poster presentation, 2022